

RIGA TECHNICAL UNIVERSITY
Faculty of Power and Electrical Engineering
Institute of Computerized Control of Electrical Technology

Artis Riepnieks

Doctoral Student of the Study Programme “Computerized Control of Electrical
Technology”

**PARAMETER ESTIMATION AND SIGNAL
MODELLING FOR PHASOR
MEASUREMENT UNITS/ PARAMETRU
APRĒĶINI UN ELEKTRISKO SIGNĀLU
MODELĒŠANA VEKTORU MĒRIEKĀRTĀM**

Doctoral Thesis

Scientific supervisor
Professor *Dr. habil. sc. ing.*
Leonīds Ribickis

Scientific advisor
Dr. sc. ing.
Harold Kirkham

Riga 2018

DOCTORAL THESIS PROPOSED TO RIGA TECHNICAL UNIVERSITY FOR THE PROMOTION TO THE SCIENTIFIC DEGREE OF DOCTOR OF ENGINEERING SCIENCES

To be granted the scientific degree of Doctor of Engineering Sciences, the present Doctoral Thesis has been submitted for the defense at the open meeting of RTU Promotion Council on December 7, 2018 at the Faculty of Power and Electrical Engineering of Riga Technical University, Azenes street 12 k-1, room 212.

OFFICIAL REVIEWERS

Professor *Dr. sc. ing.* Oskars Krievs
Riga Technical University

Research engineer *Dr.* James Follum
Pacific Northwest National Laboratory, USA

Dr. sc. ing. Antons Kutjuns
Riga Technical University

DECLARATION OF ACADEMIC INTEGRITY

I hereby declare that the Doctoral Thesis submitted for the review to Riga Technical University for the promotion to the scientific degree of Doctor of Engineering Sciences is my own. I confirm that this Doctoral Thesis had not been submitted to any other university for the promotion to a scientific degree.

Artis Riepnieks (signature)

Date:

The Doctoral Thesis has been written in English. It consists of an Introduction; 5 chapters; Conclusion; 58 figures; 2 tables; 2 annexes; the total number of pages is 91. The Bibliography contains 60 titles.

Abstract

The main research objective is power grid and phasor measurement units.

It is posited that the act of measuring the various parameters of signal is the same to solving the equation for the chosen mathematical model. Essentially is a fitting problem in mathematics. The equation is a model of what metrologists term the measurand, the name given to the quantity to be measured, and the measurement equipment must be designed around it. The equation being fit is a model based on the “physics” of the signal and natural phenomenon behind it. Regardless of exactly how the measurement is made, a metric defined and called the Goodness of Fit allows the measuring system to comment on the match between the signal it is observing and the model. The metric is based on the residuals, the differences between the signal itself and the value calculated from the result of measurement. Results from real-world phasor measurement units and real-world signals illustrate that the equation of the PMU is well solved during steady conditions. The effects of a fault in the transmission system is analyzed on the Goodness of Fit metric for a PMU.

This work addresses how to deal with non-stationary power signals. Firstly, to measure a time varying signal, in a world of digital measurements, the relationship between the sampling window of the measurement system and the rate at which the signal is varying must be addressed. In this work several changing-frequency cases are examined. It is shown that the parameters of the AC signal can be found by curve-fitting. A working proof-of-concept signal estimator is shown and realized in the MATLAB environment. Lessons can be drawn about the role of different noises in measurement and about the very meaning of the result. Statistical tools, such as Allan variance are used to examine the stability of performance for estimator, as well as noise influence on estimation process.

A new statistical analysis tool is experimentally shown to be applicable to digital measurements, called “sampling variance”. By varying sampling rate, it is shown that an optimum exists for smallest parameter variance depending on noise type.

The Doctoral Thesis has been written in English. It consists of an Introduction; 5 Chapters; Conclusion; 58 figures; 2 tables; 3 annexes; the total number of pages is 91. The Bibliography contains 60 titles

Anotācija

Promocijas darba galvenais pētījuma objekts ir elektroapgādes sistēma un vektoru mērījumu iekārtas.

Šajā darbā tiek parādīts, ka dažādu signāla parametru mērīšanas process ir tas pats, kas atrisināt izvēlēta matemātiskā modeļa vienādojumu. Būtībā to var apskatīt kā līknes parametru noteikšanas problēmu matemātikā. Vienādojums šajā gadījumā ir tas, ko metrologi apzīmē kā mērāmo vērtību, un mērīšanas iekārta ir jāizstrādā ap to. Vienādojums, kura vērtības tiek piemērotas līknei, ir nekas cits kā modelis, kas balstīts uz signāla "fiziku". Neatkarīgi no tā, kā tieši mērīšana tiek veikta, tiek piedāvāta metrika, kas definēta un nosaukta kā "*Goodness of Fit*", ļauj mērīšanas sistēmai sniegt komentārus par atbilstību starp novēroto signālu un konceptuālo modeli. Metrikas pamatā ir starpības, atšķirības starp novērotā signāla vērtībām un vērtībām, kas aprēķinātas no mērījuma rezultāta. Rezultāti no uzstādītām reālām rotējošā vektora (*phasor*) mērījumu iekārtām (PMU) un reāliem signāliem parāda, ka šīs iekārtas, lai arī to neapzinoties, atrisina rotējošā vektora vienādojumu. PMU metrikas iespējas tiek demonstrētas izmantojot reālas pārraides sistēmas datus, tai skaitā līnijas bojājuma laikā.

Šajā darbā apskatīts, kā rīkoties ar nestacionāriem energosistēmas signāliem. Pirmkārt, lai izmērītu laikā mainīgu signālu, izmantojot digitālos mērījumus, ir jāatrisina saikne starp mērīšanas sistēmas mērījumu logu ilgumu un signāla parametru mainīšanas ātrumu. Šajā darbā tiek izskatīti vairāki mainīgas frekvences gadījumi. Ir parādīts, kā AC signāla parametrus var atrast ar līknes montāžu. Izstrādāts līknes montāžas matemātiskais koncepts, kas realizēts MATLAB vidē. No iegūtajiem rezultātiem tiek izdarīti secinājumi par dažādu trokšņu nozīmi mērījumos un par rezultāta patieso nozīmi. Tiek pielietoti dažādi statistikas rīki, tai skaitā, Allana dispersiju, kas izmantota, lai pārbaudītu koncepta veikspējas stabilitāti, kā arī trokšņu ietekmi uz mērījumu procesu.

Eksperimentāli tiek pierādīts, ka jauns statistiskās analīzes rīks, kas nosaukts par "diskretizācijas dispersiju" ir piemērots digitālajiem mērījumiem. Mainot signāla paraugu ņemšanas frekvenci, tiek parādīts, ka pastāv vizuālais parametru novirzes punkts, kas atkarīgs no traucējumu veida.

Doktora promocijas darbs ir angļu valodā. Tam ir šādas sadaļas: Ievads, 5 nodaļas, Secinājumi, 58 attēli, 2 tabulas, 3 pielikumi un kopējas lappušu skaits ir 91. Literatūras sarakstā minēti 60 literatūras avoti.

Acknowledgments

I want to dedicate this work to my daughter **Skarleta** and my family to whom I owe the time and motivation to finish what had been started.

Immense thanks to Dr. **Harold Kirkham** from *Pacific Northwest National Laboratory* for overseeing the main research direction and for many captivating discussions that I value the most.

Thanks to Dr. **Leonids Ribickis** for the support in study programme and supervision of the thesis work. Thanks to **Alex McEachern** of Power Standards Laboratory for providing interesting data for analysis.

Abbreviations

IEEE	Institute of Electrical and Electronics Engineers
PMU	Phasor Measurement Unit
SEMPR	Signal Estimation by Minimizing Parameter Residuals
GoF	Goodness of Fit
ALF	Apparent local frequency
AC	Alternating Current
SCADA	Supervisory Control And Data Acquisition
UTC	Coordinated Universal Time
FIDVR	Fault Induced Delayed Voltage Recovery
GPS	Global Positioning System
A/D	Analog to Digital
ROCOF	Rate Of Change Of Frequency
ROCOA	Rate Of Change Of Amplitude
DFT	Discrete Fourier Transform
TVE	Total Vector Error
RMS	Root Mean Square
DC	Direct Current
EHV	Extra High Voltage

Table of Figures

Figure 1.1 Calibration block diagram	16
Figure 2.1 Voltage angle difference oscillations Dortmund-Bucharest [21].....	18
Figure 2.2 Phasor angle measurements across power system.....	19
Figure 2.3 Sine-wave representation (a) Sine-wave (b) Phasor representation.....	20
Figure 2.4 Macrodyne Inc. Developed PMU “Model 1690” (www.macrodyneusa.com)	22
Figure 2.5 Main functional blocks of a PMU	22
Figure 2.6 Total Vector Error visual representation	24
Figure 2.7 Linear frequency ramp test signal [2].....	25
Figure 2.8 TVE calculated for the linear frequency ramp test [2].....	25
Figure 3.1 Signal with increasing frequency [11].....	28
Figure 3.2 Measurement system for digital measurements	30
Figure 3.3 Generated point-on-wave synthetic data input.....	32
Figure 3.4 Generated point-on-wave synthetic input data for the model with non-zero ROCOF and ROCOA	33
Figure 3.5 Residuals from reconstructed point-on-wave data subtraction from the input data.....	36
Figure 3.6 Residuals by subtracting reconstructed phasor point-on-wave data from the input data.....	36
Figure 3.7 A 180 degree phase jump in the input signal	37
Figure 3.8 Input signal with step change in phase and its estimated signal.....	38
Figure 3.9 Residuals from estimated signal and input signal with 180 degree phase jump	39
Figure 4.1 Fundamental frequency and 5th harmonic	41
Figure 4.2 Harmonic distorted signal.....	42
Figure 4.3 Normally distributed Gaussian white noise.....	42
Figure 4.4 Distorted (noise plus harmonics) input signal	43
Figure 4.5 Distorted input signal	44
Figure 4.6 Reconstructed oscillography along with the signal estimate.....	45
Figure 4.7 Residuals from estimation compared to the noise signal	46
Figure 4.8 Measurements for Allan variance calculation [43]	47
Figure 4.9 Deviation as a function of measurement length [7].....	49
Figure 4.10 Allan variance for amplitude variable as a function of measurement window length.....	50
Figure 4.11 Allan variance for frequency variable as a function of measurement window length.....	50
Figure 4.12 The Allan variance of the amplitude values as a function of measurement window length for different noise amplitudes	51
Figure 4.13 The Allan variance of the frequency values as a function of measurement window length for different noise amplitudes	51
Figure 4.14 The Allan variance of the phase values as a function of measurement window length for different noise amplitudes	52

Figure 4.15 The Allan variance of the rate of change of frequency values as a function of measurement window length for different noise amplitudes.....	53
Figure 4.16 Estimated frequency with 5% added white Gaussian noise	54
Figure 4.17 Estimated ROCOF with 5% added white Gaussian noise and measurement window of 50 cycles	54
Figure 4.18 Allan variance of phase measurement affected by different levels of White Gaussian and Brownian noises as a function of window length.....	55
Figure 4.19 The change of amplitude estimation variance by different types of noises for differently sized measurement windows	56
Figure 4.20 The change of frequency estimation variance by different types of noises for differently sized measurement windows	57
Figure 4.21 The change of phase estimation variance by different types of noises for differently sized measurement windows.....	57
Figure 4.22 The change of ROCOF estimation variance by different types of noises for differently sized measurement windows	58
Figure 4.23 Graph of the function $f(x) = (e^{2x} - 1)x^{-2}$. The variance of the estimate α using N values with the spacing h is $\alpha^2 f(\alpha h)/N$. [53].....	61
Figure 4.24 Sampling rate variance for Amplitude estimation.....	62
Figure 5.1 Fault in 345kV EHV three phase system	63
Figure 5.2 PMU reconstructed signal comparison with observed oscillography data.....	64
Figure 5.3 Residuals for PMU reconstructed signal and observed oscillography	64
Figure 5.4 Goodness of Fit for 60 measurements with corresponding current measurements for phase C	65
Figure 5.5 PMU reconstructed signal comparison with observed oscillography data during fault in phase C	65
Figure 5.6 Fault in EHV system phase C, over 4 nominal cycles	66
Figure 5.7 GoF calculation for SEMPR measurements compared to GoF calculations from commercial PMU declared values	67
Figure 5.8 SEMPR algorithm reconstruction along with PMU reconstruction and real oscillography data	68
Figure 5.9 SEMPR and PMU measurement residuals during fault measurement.....	68
Figure 5.10 4-cycle measurement window measurements for data including EHV line fault	69
Figure 5.11 2-cycle measurement window measurements for data including EHV line fault	70
Figure 5.12 Single-cycle measurement window measurements for data including EHV line fault	70
Figure 5.13 Half-cycle measurement window measurements for data including EHV line fault	71
Figure 5.14 uPMU sampled data in MV distribution system	72
Figure 5.15 Spectrum of the uPMU sampled data.....	72
Figure 5.16 Allan variance for distribution network frequency measurements.....	73

Contents

Introduction.....	10
1 Analysis of different mathematical models for real world representation	12
1.1 Carnap equation and model.....	12
1.2 Rutman models.....	14
1.3 Kirkham model.....	15
2 Synchronized phasor measurements in transmission network	18
2.1 Model of a phasor.....	20
2.2 Synchro-phasor measurement units	21
2.3 PMU limitations	24
3 Theoretical background for phasor-like measurements.....	28
3.1 Kirkham equation.....	29
3.2 Principles of a digital measurement	30
3.3 Proof of concept	31
3.3.1 Input data	32
3.3.2 Measurement method.....	33
3.3.3 Output	35
3.3.4 Goodness of Fit.....	35
4 Analysis of the phasor-like model limitations	40
4.1 Noise types and their effects	40
4.2 Noise effect on the model.....	44
4.3 Allan variance	47
4.4 Sampling variance	59
5 Experimental data analysis	63
5.1 Real data estimation vs the models	66
5.2 Real data variance analysis	69
6 Conclusions	73
7 Annexes	77
8 References	87

Introduction

While enjoying wine and contemplating why phasor measurement units for transmission systems struggle to meet requirements set out by IEEE [1] Dr. Kirkham had a novel idea. In 2015 I was introduced with his idea that the act of making a measurement is actually the same as solving a mathematical equation. Consequently, an incomplete equation would give inaccurate measurement. The concept can be proved, and in 2015 we set out to do just that.

It became clear that one of the most important and trusted measurement devices for high and extra-high voltage alternating current transmission systems may have an incomplete mathematical model. IEEE even gave allowance to skip reporting measurements during signal transitions [2]. This doesn't seem right.

The idea for measurement as solving an equation gives freedom to define the model and therefore define the equations and measurands according to our best understanding of reality. Models in this case are very important and it appears that Phasor Measurement Units (PMU) during the moments we need the measurements the most – system faults - struggle to make sense of the reality with chosen model. Just as a reminder PMUs currently play a very important part in a modern transmission (recently also distribution [3]) system and helps to keep lights on.

I was very lucky to work with Dr. Kirkham during year 2015 and 2016 at Pacific Northwest National Laboratory, Richland, USA where we designed a mathematical proof of concept for an intelligent measurement. At first the priority was to find the model for instantaneous frequency of the power system that is essentially the main purpose for the PMU – to indicate sudden changes in system frequency. This work led to other findings and during the productive work together a working proof-of-concept solution, called SEMPR (Signal Estimation by Minimizing Parameter Residuals) was designed and put to the test with synthetic as well as real data. Since SEMPR is time domain calculation with complete independence between measurements, it is important to show, that calculation (or parts of calculation involving Goodness of Fit) can be done by any PMU. Joint work resulted in numerous conference publications, transactions paper and a report [4] [5] [6] [3] [7] [8] [9] [10] [11]. Interested reader is sincerely encouraged to go through the published work first, before reading this thesis as it is a continuation and unpublished extension of the current work.

First chapter deals with philosophical questions and basis for the non-stationary power system waveform measurements. Nature must be separated from the conceptual models in ones mind, while keeping the model tractable and related to nature. Models can be re-adjusted, but nature can't.

Second chapter focuses on phasor measurement units, mathematical model underneath, and their use in power system synchronized measurements. Model limitations have been indicated and possible solutions offered.

Third chapter shows the mathematical and developed practical proof-of-concept for Kirkham equation-based model for phasor-like measurements in power system (Signal Estimation by Minimizing Parameter Residuals).

In fourth chapter the limitations for SEMPR are explored with various synthetic signals, containing variations of noises and harmonics. Statistical analysis methods are implemented and sampling variance is introduced. Chapter provides first experimental results on sampling variance for possible uses in real-world applications.

Fifth chapter contains results from real-world signals and PMU measurements, including a fault in Extra-High Voltage network. It is shown that SEMPR in general performs better with measurements over the fault sampled data than PMU. Results of statistical analysis is provided for real-world Medium Voltage distribution network signal.

This work is on 91 pages, has 58 figures, 2 tables, 3 annexes and 60 references.

1 Analysis of different mathematical models for real world representation

Curiosity has been one of the most beneficial characteristics of our society. Our constant urge to ask questions has led to scientific discoveries and great accomplishments. At the very basis of each question is our perception of things we observe. Note that the perceptions may be different from person to person and not easily comparable. This is where mathematics comes to aid and can describe our perceived model in our heads in a very definitive way.

Mathematical models are our constructions of the reality and for most cases can be branded as “our best guess” while the chase for universal model for explanation of the universe is still on. One of our best guesses and Standard model [12] is incomplete and could be part of bigger picture. Nonetheless, we have come a long way since Pythagoras around 500 BCE was one of the first to begin to describe Earth as spherical and a student of Plato – Eudoxus put the Earth at the center of the Universe and described first known mathematical model for the celestial motions [13]. This model was then advanced by Greek philosopher Aristotle, but eventually dismantled by Nicolaus Copernicus in 1543. For understanding how things work, models are important.

Like with Aristotle and Copernicus models, both are based on observations and meant to explain celestial motions, but the outcome is very different. Here the scientific method is essential. An empirical method must be provided to root the model in reality.

1.1 Carnap equation and model

Rudolf Carnap was a German-born American philosopher and considered one of the giants among twentieth century philosophers. His work and contribution to inductive logic is considered one of the greatest achievements of modern philosophy [14].

Large part of his early work is related to philosophy of physics and experimental method. The experimental method (scientific method) allows us to take action, instead of being just onlookers. Instead of waiting for a situation where observation could happen we can purposely make such situation, essentially make an experiment.

The most relevant notion to begin with is the Carnap quantitative language of a measurement, or in other words - labeling for different models. A good example is given in [15] with spatial length. Consider two bodies with length, for example pieces of wood a and b . If they are combined so that they are end to end lying in a straight line the new physical entity is now a combination of two objects and have length that is the

sum of the lengths of a and b . This sounds like additive rule for length. Unfortunately, quite often this rule is not satisfactory. As Carnap observes, this is a very poor way to formulate a rule, main issue being that the word “add” is being used twice in the same equations, but with very different meanings. At first, it’s used for joining together two physical objects and then it’s used to describe an arithmetical operation. It is not possible to arithmetically add two lines and expression

$$L(a + b) = L(a) + L(b) , \quad (1)$$

where L is the length of the two pieces, is erroneous. The second symbol “+” expresses the arithmetical operation of adding, but the first one does not. You can add two numbers, but you cannot add two bits of wood as they are physical objects in space. In this sense the first symbol “+” denotes the physical operation of combining and Carnap really stresses out the difference between the two worlds – physical and mathematical. The symbol for physical joining operation “ \circ ” is then introduced. Correct way of expressing the joining of two lines then is

$$L(a \circ b) = L(a) + L(b) . \quad (2)$$

It is obvious that the left part of the equation denotes the real, physical world and the right part is the conceptual or mathematical one. The “=” is the bridge between them and realized as the act of measurement. By the act of measuring we can transfer from operations with physical objects to mathematical operations in the conceptual world. The “=” of course is true only if we can know the actual true value by measuring the thing and whether “ \approx ” would be more appropriate, is a conversation topic on its own.

By this point we can talk about the characteristics of a wave function and its representation in our conceptual minds. Every periodic function has a frequency parameter, but frequency by definition “number of occurrences per unit of time” is something existing in real world as swinging pendulum or celestial cycles. Once we cross the “=” in Carnap equation (2) it becomes a variable in an equation of a wave function. There is a large difference and we should avoid confusing them at all times. For the purpose of this work the term “frequency” denotes second variable in wave function (symbol ω) and the physical property of this number should be put aside, since there are questions like:

- What is the frequency when frequency is changing?
- What is the frequency for a quarter of a cycle signal?

In this sense in this work “frequency” (if not said otherwise) is only true for the measurement window and is a parameter in an equation for a mathematical model. During work it was proposed to switch from term “frequency” to “apparent local frequency (ALF)” (apparent, because conceptual, local, because true only for measurement window), but it was never widely used.

1.2 Rutman models

Jacques Rutman is a French scientist who has contributed greatly to precision oscillators in clocks and frequency stability measurements. Keeping in mind the distinction between the nature and our conceptual world J. Rutman put it this way:

“... models are used to represent the physical world which is so complex that many details are ignored in the model: otherwise, the latter would become intractable. On the other hand, properties that have no direct meaningful counterparts in the real world have to be included in the model to make it tractable (stationarity of random processes is a well-known example).” [16]

So, we are quite free to add or remove parameters and assumptions to our conceptual models of reality, but have to always keep in mind that it does not change the reality itself, just our understanding. If something changes in nature, we have to accommodate in our models, otherwise our knowledge of the phenomenon being observed will be completely wrong, yet measurement can still be very accurate.

In [17] J. Rutman points out that:

“At first, it is important to emphasize on the fact that the two following facets are often confused:

- *The real world, with its physical devices, measurement apparatus, experimental results derived from reading meters, counters, dial settings and so on.*
- *The mathematical model, with the means and rules for operating with the symbols introduced in it.”*

The mathematical model of an oscillator is given in [17]:

$$V(t) = [V_0 + \xi(t)] \sin[2\pi\nu_0 t + \varphi(t)] , \quad (3)$$

where V_0 is nominal amplitude, ν_0 is nominal frequency, $\xi(t)$ is random amplitude noise and $\varphi(t)$ is random phase noise.

So, what is the frequency when the frequency is changing? Instantaneous frequency?

Instantaneous angular frequency for (3) is

$$\omega(t) = \frac{d}{dt}(\omega_0 t + \varphi(t)) = \omega_0 + \frac{d\varphi(t)}{dt} , \quad (4)$$

where $\dot{\varphi}(t) = \frac{d\varphi(t)}{dt}$ is a random frequency fluctuations around the ideal value ω_0 . But for model tractability in physical world (Carnap equation left part) the mathematics get very tricky, pointed out by Rutman in [17].

There is stationarity problem for $\varphi(t)$ where theoretically white noise in oscillators leads to phase diffusion process similar to Brownian motion. In this case it becomes impossible to introduce exact correlation function or a spectral density of the phase. Since a lot of random processes has no derivative function, the existence $\dot{\varphi}(t)$ is at question. Even if the physical interpretation seems obvious, is not always mathematically defined. As Rutman concludes, one must be very careful when dealing with phase and frequency noises, since it may lead to a use of non-existent quantities. In this work SEMPR is made to operate with frequency, phase, and amplitude noises, but it is done controllably keeping in mind the physical implications.

For physical sense for this work Rutman states in [17] that essentially instantaneous frequency for Carnap left side of the equation can never be instantaneous since it always involves a finite averaging interval τ . The notion of frequency for a dot on a wave function is simply not possible and the same distinction must be drawn between mathematical frequency (e.g. ALF) and physical frequency of a periodical wave.

1.3 Kirkham model

The question about what the frequency is when the frequency is changing resulted in new ideas and research in phasor-like measurements [11]. It did not stop there, and many philosophical questions have been discussed. Interested reader is referred to Annex No. 3 for frequency measurand discussion.

Consider equation (2) and separation of nature and conceptual model of nature. In [18] Claude Shannon admits that frequently the messages sent over telecommunication channel has meaning that is, they refer to or are correlated. He then went on to discard this notion as this, in his words, is not part of the engineering problem for the communication channel he was considering. It is Dr. Kirkham's idea to show that the "message" coming from a measuring device has "meaning" and it must not be ignored. The correlation to the nature in left side of Carnap equation should be kept. The equal sign in the equation (2) is the link between conceptual and real worlds, but it must be approached carefully as it does not mean "is the same as", instead it should be interpreted as "is the same value as". Therefore, the physical frequency of repeating oscillations is not the same as the value for the frequency in a mathematical model, it's just a representation.

The same stands true not only for measurement, but also for signal generation. Dr. Kirkham shows that those are practically the same just in different directions in Carnap equation,

$$\begin{array}{c}
 \xrightarrow{\text{signal generation}} \\
 X(a \circ b) = X(a) + X(b) \\
 \xleftarrow{\text{measurement}}
 \end{array}
 \tag{5}$$

where measurement is an act of solving an equation for mathematical model values, but the process of signal generation moves information from the mathematical model into physical world. As Kirkham indicates, calibration, of course involves both. The calibration block diagram is given in [11]

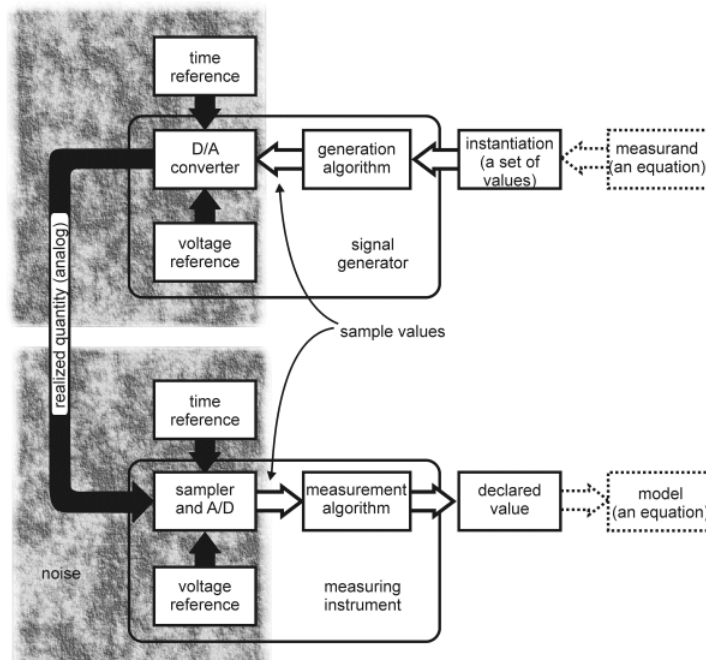


Figure 1.1 Calibration block diagram

In Figure 1.1 the calibration corresponds to Carnap equation very well. On the left side there are real-world non-perfect and noisy signals, and on the right side is the conceptual mathematical world, that in both cases (measurement and generation) contains some mathematical models, made by our understanding of physics and mathematics.

Coming from this work is the notion that mathematical models for measurements (and signal generation) are extremely important if one wants to keep the correlation to actual real-world signals. The majority of work then has been in the direction of AC sinusoidal signals in power transmission systems and phasor measurement units as the main measuring devices. Real-world signals usually are not stationary and power system AC waveform is not any different. So, if the signal in real-world is changing, so should our conceptual model for this signal. This is where a slight

change to a phasor equation was made and Kirkham introduces rate of change of amplitude and rate of change of frequency in the model (15) for phasor measurement units.

2 Synchronized phasor measurements in transmission network

Synchronized phasor measurements are becoming one of the most vital measurements of a modern power system. This information, based on stream of measurements, can tell a lot about system dynamics and system stability ensuring that lights stay on.

There are many control and supervision systems already in place for power systems (like SCADA), but there are still very strong incentives to introduce solutions that are faster and more insightful. With SCADA the measurements are captured every 4 seconds or so and from different areas they are not captured at the exact same time. If monitored for only voltage, power and reactive power, the solution can be satisfactory because these things usually don't change very suddenly (unless large disturbance). However, system monitoring is essential during large disturbances and transient processes. In order to capture system dynamics and for fast real-time control/supervision faster capture periods and synchronized data is essential [19].

Synchronized phasor measurements mean that all measurements are using the same time reference and are synchronized with UTC (Coordinated Universal Time) using GPS (Global Positioning System) clocks [20]. This way all measurements can be drawn on one single axis and shown frame by frame. With fast measuring rate (25 measurements per second in 50 Hz system and 30 measurements per second in 60 Hz system) system dynamics begin to appear (Figure 2.1) and it is possible to monitor system transient processes. Now, by using synchronized measurements it is possible to discover blackouts, line tripping, generation unit dropping from network, FIDVR (Fault Induced Delayed Voltage Recovery) and other transient processes in real time. With resilient and fast telecommunications network, it is also possible to control the power system elements in real time to apply counter measures and keep the system in balance.



Figure 2.1 Voltage angle difference oscillations Dortmund-Bucharest [21]

The thought behind using synchro-phasors for system state estimation is rooted in notion that sine-wave between two adjacent buses will change the phase angle depending on the load as seen in Figure 2.1. By measuring synchronized phasors at both instances the P flow can be then computed.

As shown in Figure 2.2 it makes sense to measure phasor angle across all parts of large interconnections to monitor system and individual line connection performance. In this case drop of generation unit or line tripping will be immediately observed in corresponding phasor measurements. Information gathered from all measurements simultaneously and synchronized to UTC can help to monitor system dynamics (oscillations), improve system models and protection gear settings as well as react to system transient processes and prevent possible blackouts.

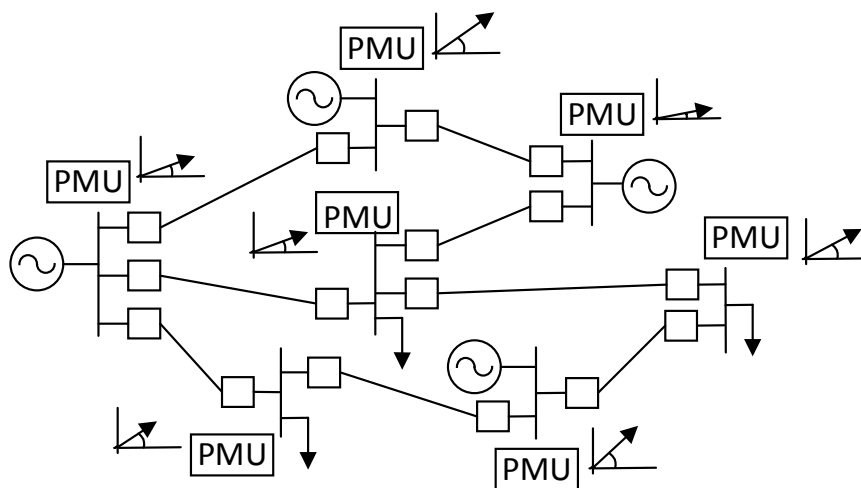


Figure 2.2 Phasor angle measurements across power system

Because the main characteristics of interest in a power system usually are voltage, frequency and their stability, phasors are used for much more than just line load estimation. One implementation lies in control and protection domain, where phasors can be very useful [22] [23]. The system must be at equilibrium between generated and consumed power at all times in order to ensure stable voltage levels and system frequency. Stability depends on three factors: rotor-angle stability, frequency stability and voltage stability. With the evolving grid it is challenging to monitor and maintain all the parameters. Increasing complexity and interconnectivity of a modern power system [24] as well as larger penetration of distributed renewable energy sources [25] can create instability of the power system frequency and cause oscillations between different areas. These usually are low frequency oscillations, like for example European interconnected network including 28 countries oscillates at around 0.15Hz (Athens-Stuttgart-Seville-Algiers) [24]. System oscillations at some circumstances can cause severe system instability, falling out of synchronism and blackouts [26].

2.1 Model of a phasor

In order to make power systems tractable it is necessary to use mathematical models and the model of a sinusoid is a good representation at a first glance of a stable power system. It is then possible to express power system signal mathematically as a sinusoid equation [27]:

$$x(t) = X_m \cos(\omega t + \varphi) \quad (6)$$

where X_m is amplitude, ω is frequency and φ is phase. This model includes all information to reconstruct a sinewave. It is customary to imagine a diagram representing this equation. The time is set to zero, and a line drawn at angle φ to the horizontal, with (scaled) length X_m . This line was originally termed a vector, and later became called a phasor.

Arun Phadke, J. Thorp and M. Adamiak proposed a new idea in their 1983 paper on how to measure frequency really fast and without counting signal zero-crossings [28] by using model of a phasor. In their scheme, the two parameters are known as a synchrophasor. A mathematician might call them the stationary phasor, since by setting the time to zero, the effect of frequency is removed. Frequency is regarded as a separate quantity for measurement. Consider the exponential notation representing the sinusoid:

$$X_m \operatorname{Re}[e^{j(\omega t + \varphi)}] = X_m \operatorname{Re}[X_m e^{j(\omega t)} + e^{j(\varphi)}] . \quad (7)$$

In power applications, it is customary to omit the *Re* notation and to omit the frequency term, so that a sinusoidal input signal as in (6) is written

$$x(t) = X_m e^{j\varphi} . \quad (8)$$

Note that the simplified equation of the sinusoid does not include the frequency. It includes only the stationary phasor. Also showed in Figure 2.3 in time domain (a) and complex domain (b).

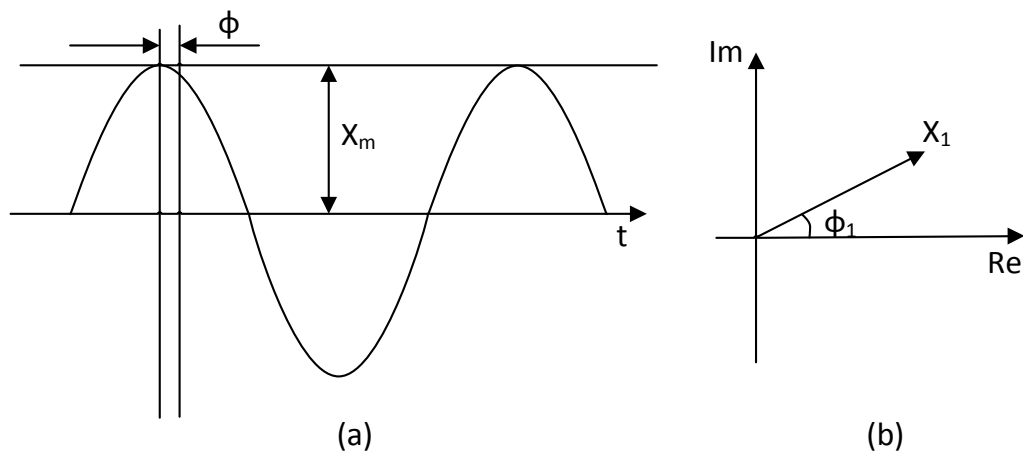


Figure 2.3 Sine-wave representation (a) Sine-wave (b) Phasor representation

All the information about the stationary signal is there: amplitude, frequency, and phase angle. Measuring amplitude is not so challenging but measuring phase angle and frequency is a hard thing to do (for real time applications). As shown by A. Phadke *et. al.* in [28] it is possible to measure the difference in the phase angles between the recursive phase measurements and, by doing that, find the change in the frequency:

$$\frac{d\psi}{dt} = \frac{\psi_r - \psi_{r-1}}{(1/50N)} \quad (9)$$

where ψ is derived from a “phase factor” $e^{j\psi_r}$, the differentiated phase angle, r is recursive measurement and N is sampling rate in samples per cycle.

Difficult measurements like frequency in real time on the power system has been a long-time interest for power engineers. A value called “rate of change of frequency” (ROCOF) was expected to be a very useful tool to indicate changes in the power system. In case of generation unit loss or line tripping, the frequency would be affected and ROCOF would indicate how fast the changes are. Then actions can be taken based on ROCOF information. From change in the frequency between two recursive measurements ROCOF can be derived,

$$\frac{df}{dt} = \frac{1}{2\pi} \frac{d^2\psi}{dt^2} \quad (10)$$

where f is the frequency.

It is important to note that the model of a phasor describes a sine-wave with static frequency and amplitude that is true from reference time to infinity of time. This is the mathematical model used in phasor measurement units (PMUs).

2.2 Synchro-phasor measurement units

From the idea proposed in 1983 [28] it took 5 years for developing a PMU prototype [21] in 1988 at Virginia Tech, USA and in 1992 first commercial PMU was produced at Macrodyne Inc., USA (Model 1690). In 1995 the first standard was developed, and most recent update was released in 2014 [1] to change performance requirements.



Figure 2.4 Macrodyne Inc. Developed PMU “Model 1690” (www.macrodyneusa.com)

PMU (in Figure 2.4) is a time synchronized measuring device reporting estimates of positive sequence voltage amplitude and phase angle, local frequency, and rate of change of frequency. It is previously shown that measurements are done only for amplitude and phase angle. The other values are then calculated based on differentiation.

The input for any PMU is a sine wave signal that gets filtered usually with a low-pass filter to get rid of possible harmonics and noise on the signal that can cause aliasing. Then it is turned into a digital signal by sampling in A/D converter and creating point-on-wave data stream. The data stream is synchronized with UTC signal that is received from GPS receiver. Using the data and reference time ($t=0$) processing unit can calculate the phase angle and positive sequence voltages and currents (Figure 2.5). Based on these measurements local frequency and rate of change of frequency is determined.

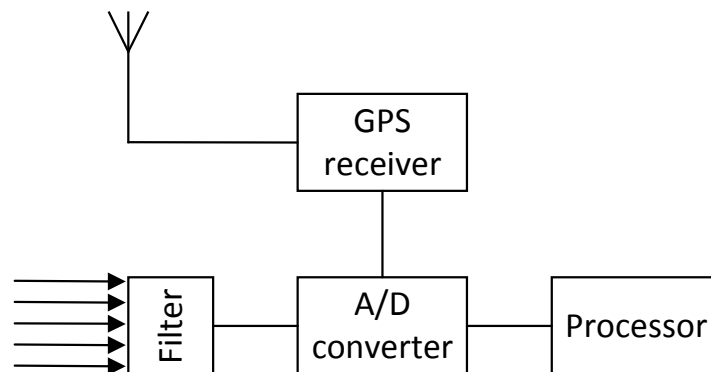


Figure 2.5 Main functional blocks of a PMU

Based on performance requirements posed by [27] and [1] all PMUs can be sorted in two categories: P and M type. P type PMUs usually are used for protection applications and their requirements include very fast reporting times (at least 25 measurements per second). M type requirements are more intended to deal with adversely aliased signals and do not require blazingly fast reporting speeds e.g.

response time for ROCOF step change estimate is $14/f_0$ over P type $6/f_0$, where f_0 is the nominal frequency. Testing of PMUs is a very interesting topic to which an interested reader is forwarded to [6] and [4] for more detailed insight.

Actual measurement unit algorithms are commercial secrets for each PMU manufacturer, but in general at least some parts of digital signal processing are taking place in each and every one of them. Discrete Furrier Transform (DFT) is calculated to transfer from time domain to frequency domain. Seemingly logic thing to do because frequency and rate of change of it is what we are really after. The DFT is done according to [20]

$$x = \frac{\sqrt{2}}{N} \sum_{k=1}^N x_k \varepsilon^{\frac{-j2k\pi}{N}}, \quad (11)$$

where N is total number of samples in one period of the signal, x is the phasor and x_k is the point-on-wave sample.

The main feature of frequency-domain based calculations as described by Arun Phadke in [20] is that it produces the positive sequence phasor

$$x_1 = |x_1| \varepsilon^{j\varphi}, \quad (12)$$

with an angular velocity exactly corresponding to the difference between system reference frequency and observed frequency. The system frequency is then

$$\omega = \omega_0 + \frac{d\varphi_1}{dt}. \quad (13)$$

While details of the phasor calculation techniques in PMUs are unknown to the public, for sure they include common key points:

- Input signal is filtered;
- Sampling rates can vary greatly (from 24 samples to 512 samples per cycle [29]);
- DFT is calculated;
- Sampling may be synchronized with the UTC clock or the signal itself;
- Phase angle differentiation is performed to calculate system parameters;
- Parameters are time-stamped and forwarded to a data concentrator.

The outcome information from the PMU is 3 phase positive sequence voltage magnitude and angle, 3 phase positive sequence current magnitude and angle, local frequency (as deviation from nominal), Rate of change of frequency, additional defined analog or digital signals (like transducer values, relay statuses or other flags). Since all this information comes from phasors, the accuracy of a PMU measurement is expressed in parts per unit as TVE (Total Vector Error) of a “perfect theoretical phasor” [30]. TVE is described in the standard [27]:

$$TVE(n) = \sqrt{\frac{(\hat{X}_r(n) - X_r(n))^2 + (\hat{X}_i(n) - X_i(n))^2}{(X_r(n))^2 + (X_i(n))^2}}, \quad (14)$$

where $\hat{X}_r(n)$ and $\hat{X}_i(n)$ are the sequences given by phasor estimates, $X_r(n)$ and $X_i(n)$ are theoretical values of the input signal at given time (n).

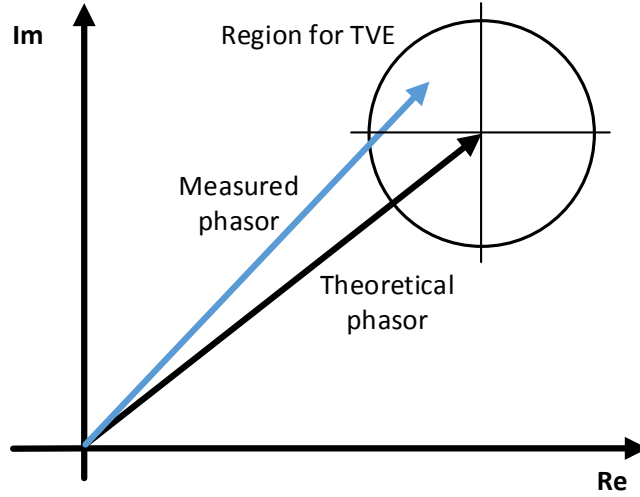


Figure 2.6 Total Vector Error visual representation

According to [1] allowed TVE for a steady state test is 1%, which means that there can be 1% difference between observed phasor and theoretical phasor.

2.3 PMU limitations

Synchrophasor measurement units have to deal with many problems and just to mention couple of them are timing and synchronization, signal filtering, noise, and sudden large disturbances in the signal.

Timing is very important in synchronized measurements. The precision requires μs precision on the clock (allowed 1% TVE error corresponds to $\pm 31\mu\text{s}$ time error in 50Hz system [1]) therefore GPS clocks (or equivalent) are essential. PMU therefore have to account for connection latency and delay of UTC signal to make synchronized A/D conversion. This becomes very important when comparing two different vendor PMUs because synchronization processes can be implemented differently (some A/D converters are phase locked to the system frequency).

Filtering the signal is necessary to solve aliasing problems and also to remove any harmonic disturbances with any out of band signals. Filtering brings a delay that has to be taken into account. Using filtering across many windows the reported value

is not entirely independent of previous, so there is a delay for reporting times because of the signal filtering [31] [32].

Basic principles of phasor measurements intend differentiation and that is a very noise sensitive operation. This puts more strain on filtering and filters distort the view of the real signal. Even with all the filtering used PMUs still struggle to measure ROCOF [4]. This was a serious issue that resulted in a standard amendment in 2014 [1] giving PMUs more achievable requirements.

Interesting PMU performance indication comes out of the G.Stenbakken and M.Zhou 2007 paper and also PMU standard amendment [1] [2]. The standard under dynamic compliance (performance during ramp of system frequency) states:

Measurements made during an exclusion interval shall not be used when determining measurement compliance. The exclusion interval is the time interval after the ramp leaves or before the ramp reaches the frequency range limit or a point where ROCOF changes.

This is curious situation. On one hand it is well known that the system frequency (therefore ROCOF) is changing all the time and at no point, it is static as the system is indeed dynamic in nature. On other hand, during testing the PMU can ignore windows when ROCOF is changing. In [2] it is experimentally showed how it looks in practice. When applying linear frequency ramp to the device under test and ignoring the transitions it is shown that TVE does not exceed 0.001%. But the graph looks silly (Figure 2.8).

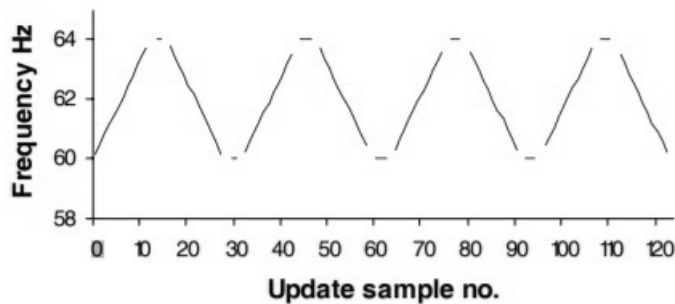


Figure 2.7 Linear frequency ramp test signal [2]

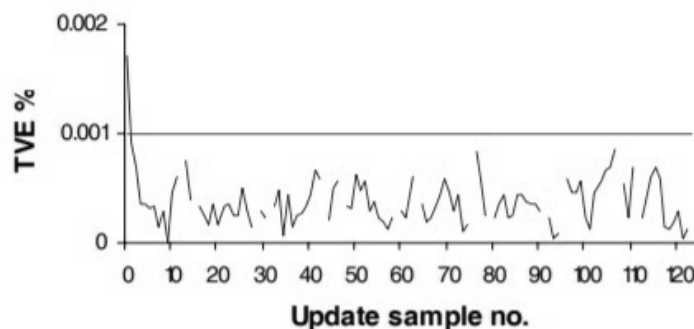


Figure 2.8 TVE calculated for the linear frequency ramp test [2]

Transitions is something that is closer investigated in [4]. It is shown that allowing for a ROCOF to change in the mathematical model (Kirkham equation) the transition process can be monitored. Of course, more investigation is needed to fully understand the implications, but at least we can look at transitions and discuss. Interested reader is referred to [4] for more detailed discussion.

This is something that needs to be looked at in more detail. When attempting to replicate the conditions PMU would face during frequency ramp testing a strange phenomenon was discovered. More details of this is described in [4] and [6].

We have to begin with right side of Carnap equation and the way the input signal is generated. This process involves modulation techniques. This is not broadly considered a problem and frequency modulation has been around a long time.

In 1946 Balthazar van der Pol presented a paper [33] in which he argued for referring to the whole cosine argument in (6) as the “phase” (nowadays term “phase” is mostly reserved to just φ). Referring to the whole cosine argument as the phase allows comparison of phases for two signals with different frequencies and express it mathematically.

A term “total phase” can be used with Ψ assigned to it. Then the (6) can be re-written as

$$x(t) = X_m \cos \Psi \quad . \quad (15)$$

Expression (15) compared to (6) is more general and doesn't require the argument to be linear function to time. This is also better representation of non-stationary signals in power systems. This is discussed more in chapter 3.1.

To define different modulation methods, van der Pol uses expression similar to (6)

$$y(t) = A \cos(\omega t + \varphi) \quad , \quad (16)$$

where A is amplitude, ω is angular frequency and φ is phase constant, but most importantly the argument of cosine function ($\omega t + \varphi$) is the phase. For example, amplitude modulation can be expressed

$$A(t) = a_0[1 + mg(t)] \quad , \quad (17)$$

where $g(t)$ is the modulation signal and m is the modulation depth coefficient. For phase modulation we can quite conveniently stick to the same technique and express modulation as

$$\varphi(t) = \varphi_0[1 + mg(t)] \quad . \quad (18)$$

For frequency modulation it would be very intuitive to use the same expression and substitute ω in

$$\omega(t) = \omega_0[1 + mg(t)] , \quad (19)$$

but van der Pol stresses it right away that such expression is erroneous and, in his words, “*lead to physical absurdity*”. For frequency modulation van der Pol reasoned rewriting the expression (16) as

$$y(t) = A \cos \left(\int_0^t \omega dt + \varphi \right) , \quad (20)$$

where the argument of cosine function is the phase $\psi(t)$.

A hint of physical absurdities is given by Boashash in [34] where he argues that when substituting (19) in (16) the phase will not comply with (18). Indeed, when the oscillating signal is calculated with multiple modulations and changes of modulation, then phase jumps in the signal start to appear. This problem, however, appears only with the transition from the conceptual world to the real world, because, just like Rutman pointed out, we disregarded a part of physical phenomena to make the model more tractable. Others have also run into this problem, but have not realized it or haven’t investigated further, like case discussed in [6].

The essence of the problem is within creation of the synthetic signal, for example, with spreadsheet. Consider creating ramping frequency signal using (19) beginning with stationary signal (rate of change of frequency is zero) at t_0 and then at some given time point t_k introduce a rate of change of frequency. From $t=0$ to $t=t_k$ spreadsheet is calculating the signal and describing a cosine waveform. At t_k the rate of change of frequency starts to change the phase. Suppose that the rate at which the frequency is changing is changing again (like in Figure 2.7) at $t=t_m$. The spreadsheet continues to produce cosine describing sample numbers, but at t_m the phase has changed from $t=t_0$ so a phase jump is created – a physical absurdity.

This problem got named “van der Pol problem” during the research. The solution is simple and for each sample calculation the calculation must be done for new frequency and phase values in each step. This comes natural for real signal generators, because then (20) would apply.

3 Theoretical background for phasor-like measurements

The classical phasor equation (6) describes a static sinusoidal signal that is true from the beginning of time till infinity. Unfortunately, this static situation is never true for real world signals, even in laboratory environment. Consider the signal in Figure 3.1.

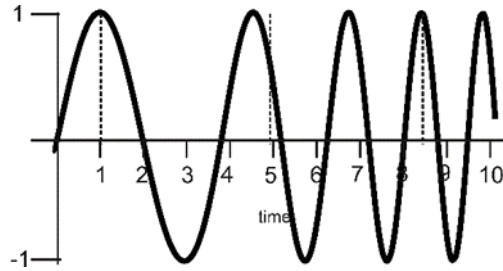


Figure 3.1 Signal with increasing frequency [11]

Let's say we need to determine the frequency of given signal. It is clear that ROCOF is nonzero and positive as the frequency (assuming that the word can somehow be interpreted in a way that applies to the signal shown) is increasing. It is clear that traditional time measurement between zero-crossings will not be useful. However, what is the frequency we should report? What is the frequency when frequency is changing? What does the "frequency" even mean in this sense? If we report one number, should it be the average frequency for a given period or instantaneous frequency at the middle of measurement window? At the end of the window?

It would be very obvious to look for "instantaneous frequency" and watch it advance, but it is worth noting that for physical measurements instantaneous frequency for just one sample of the signal cannot be defined. Any measurement requires a finite time that cannot approach zero – instantaneous frequency by definition cannot be measured [35]. We have to define a measurement window with more than one sample. This brings back the question about changing frequency (also when generating the signal [33]).

Say we obtain the average value for frequency within the measurement window. By using the value and a mathematical model of a phasor (6) it would be false representation of the real signal (model does not allow frequency to change within the window). A more suitable mathematical model is needed for representation of changing signals. As put by Boualem Boashash [34]:

Nonstationary signals in particular do not lend themselves well to decomposition into sinusoidal components. For such signals, the notion of frequency loses its effectiveness, and one needs to use a parameter which accounts for the time-varying nature of the process.

Note, that B. Boashash also tells us that a new meaning for the “frequency” parameter should be defined, because for nonstationary signals there is little sense talking about frequency.

3.1 Kirkham equation

Observing the changing nature of the real world it becomes clear that this change needs to be represented also in our mathematical models. In 2014 report [36] Harold Kirkham presented what seemed to be a novel and fundamental idea for the digital age of metrology – making a measurement is actually the same as solving an equation (mathematical model).

Consider the increasing frequency signal in Figure 3.1. There is no parameter in phasor model to accommodate that sort of frequency change over the measurement window. In the 2014 report at Pacific Northwest National Laboratory Kirkham suggested suggests modifying the equation of a phasor (6) with additional parameters that would allow the signal to change. In later work Kirkham called it a “phasor-like” equation (hereinafter in this document referred to as “Kirkham equation” as it is the foundational principle of all further work in this document):

$$x(t) = \left(X + \frac{C_X}{2}t\right) \cos \left\{ \left(\omega + \frac{C_\omega}{2}t\right)t + \left(\varphi + \frac{C_\varphi}{2}t\right) \right\}, \quad (21)$$

where each of phasors parameters are modified with coefficients C , to allow for them to change in linear manner (the simplest way of change). Since change in the signal phase cannot be distinguished from changing “frequency”, these two coefficients can be merged, and the Kirkham equation modified:

$$x(t) = \left(X' + \frac{C'_X}{2}t\right) \cos \left\{ \left(\omega' + \frac{C'_\varphi}{2} + \frac{C'_\omega}{2}t\right)t + \varphi' \right\}. \quad (22)$$

The mark to each parameter is added for indication of non-stationarity (as a difference to a phasor). Very important remark is that the linear change and the parameters of Kirkham equation applies only to a duration of measurement window (in contrast to phasor that holds true for $t=0$ to infinity).

Reconsider the signal in Figure 3.1 with the Kirkham equation. It becomes apparent that the frequency is changing while amplitude is remaining constant so the mathematical model for the measurement should be:

$$x(t) = X' \cos \left\{ \left(\omega' + \frac{C'_\omega}{2}t\right)t + \varphi' \right\}. \quad (23)$$

For this purpose, X' is the amplitude, ω' is “frequency”, C'_ω is ROCOF and φ' is phase. Mathematically, to obtain the actual values we would need to solve the equation for all the parameters. As shown by Kirkham it is exactly what we can do to make a measurement [36] [11] [37].

3.2 Principles of a digital measurement

These following principles can be applied to almost all digital measurements, but for explanation purposes and close relation to previous work, more emphasis will be put on phasor-like models and measurements.

In Kirkham equation (23) for the signal in Figure 3.1 on the left side of the equation we have the real-world signal (realized quantity) observed and then quantified by the A/D converter. On the other side we have our best guess of mathematical representation of the real-world process. It is obvious that we cannot truly measure a quantity that is not expressed in mathematical model, therefore defined in our understanding of the real world.

Digital measurement system for this is very well shown and described in [11]. In Figure 3.2 is shown the basic structure of a digital measurement system. Analog signal is fed into A/D converter and the signal is sampled according to time reference (time stamped samples) and voltage reference (sample values). The “front-end” of this system is susceptible to noise, which can affect not only the analog signal, but also time reference and voltage reference. Point-on-wave data is then processed by measurement algorithm (e.g. FFT in conventional PMUs) and declared value is presented at the end of this process. This value then must not be taken out of the context, for example, if it is “apparent frequency” in the Kirkham equation then it is true only for the measurement window and represents the second parameter in the equation (model).

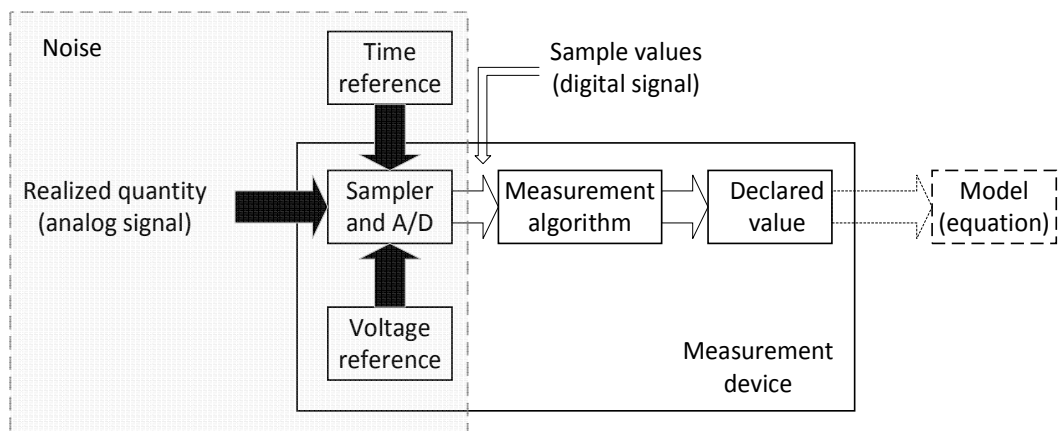


Figure 3.2 Measurement system for digital measurements

While the “front end” (grey part in Figure 3.2) is susceptible to different kind of noises (white, Gaussian, Brownian etc.) the “back-end” of the measurement system is more affected by “semantic coloration” [37] or in other words incomplete mathematical model for the measurement. In a basic sense this happens on two occasions:

- The mathematical model for the measurement is erroneous and therefore the declared values do not represent the process observed;
- The signal is affected by some unforeseen disturbance. In this case there will be no representation for it in the model and measurement algorithms, therefore this value is not only ignored by measurement, but other declared values get affected by it.

This coloration could be a DC component on the AC signal measured in accordance to (21) in which case, probably the declared value for amplitude would be altered slightly. Put it in other way, semantics is meaning, and semantic coloration is a **meaningful** mismatch between the observed reality and the model.

It becomes clear that the declared value is not the quantity of the real world we observe, but instead it is an answer to our question posed by our understanding and our instrument. The great physicist Werner Heisenberg put it this way:

“... since the measuring device has been constructed by the observer, we have to remember that what we observe is not nature itself, but nature exposed to our method of questioning” [38]

By allowing the “frequency” to change in the model we have accounted for frequency change and presumably improved our representation of the signal observed.

Using this notion, it would be possible and beneficial to implement an automatic self-calibration e.g., after transducer change [9]. This would also improve measurement accuracy and device user experience.

3.3 Proof of concept

For the proof of concept, it was authors opinion that it would be beneficial to show several different non-stationary signals and develop a workable solution to make measurements.

After realization that the act of measurement is the same as equation solving the question becomes clear: what are the values that produce the real-world signal? To find out, one method is to use curve fitting. By fitting the equation to the samples of the observed signal, could the values in the mathematical equation be found that give the best fit and therefore can account for the signal observed?

The software used, was “Mathworks Inc. MATLAB” and it was used to make a fitting method for the proof of the measurement concept. MATLAB was chosen because of ease of use and previous experience working with this software.

A number of estimator versions were built and improved in this effort. The best results until now have been produced by a least squares estimator. This minimizes the mean square residual between the signal measured and values predicted by the equation.

3.3.1 Input data

The test signal is synthetically generated by using Microsoft Excel spreadsheet. On 60Hz system the PMUs usually sample at 24 samples per nominal cycle. To retain approximate same time distribution between samples for 50 Hz system, 30 samples per nominal cycle were used.

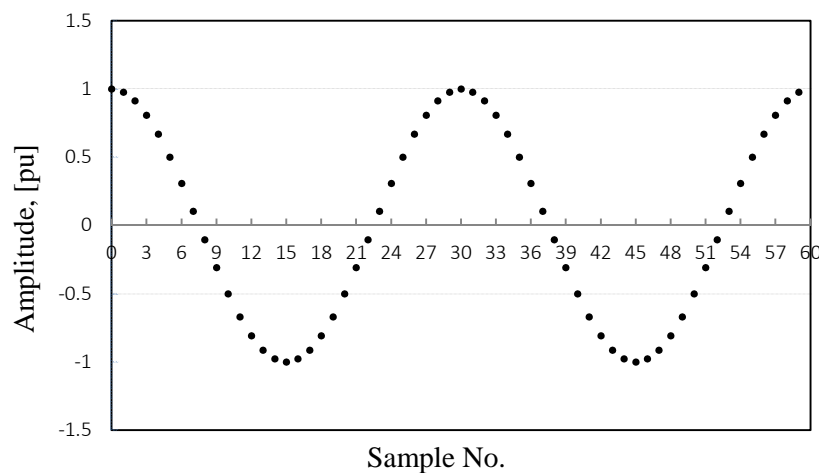


Figure 3.3 Generated point-on-wave synthetic data input

The mathematical model for the measurement is the equation (22) with added degrees of freedom for amplitude, frequency, and phase to change (compared to classical phasor) within the measurement window. The measurement window is selected to be 2 cycles, since that is the most popular window size (not accounting for signal filtering) for real P application PMUs. So, equation (22) is the mathematical representation of the signal the measurement system is supposed to analyze, and report declared values of this model. For modulated signal generation, of course, (20) is implemented.

In terms of input of information for the measurement method there is not only the mathematical model, but also a “trust region” for the variables in the equation. It is beneficial to provide the measurement algorithm, the device and also the person interpreting a measurement, with all available information about the real world we are about to explore. In this case it is known that the amplitude will not likely exceed twice

its nominal value, frequency cannot drop below 0 and exceed, say, 100 Hz. The same goes with phase as it is constrained by 2π radians. Looking at grid events suggests for ROCOF value ranging between tens to couple of hundreds of mHz/s, but for research purposes the trust region is selected wider (couple of hundreds \pm mHz/s).

For proof of the model and measurement method a signal with non-zero ROCOA (rate of change of amplitude) and ROCOF were used. ROCOA value is set to 0.1 pu/s and ROCOF is set to 3 Hz/s

Variables for the signal generating equation (22) are selected:

- Amplitude $X' = 1$ [pu]
- Rate of change of amplitude $C'_x = 0.1$ [pu/s]
- Frequency $\omega = 50$ [Hz]
- Rate of change of frequency $C'_\omega = 3$ [Hz/s]
- Phase $\varphi = 0$ [rad]

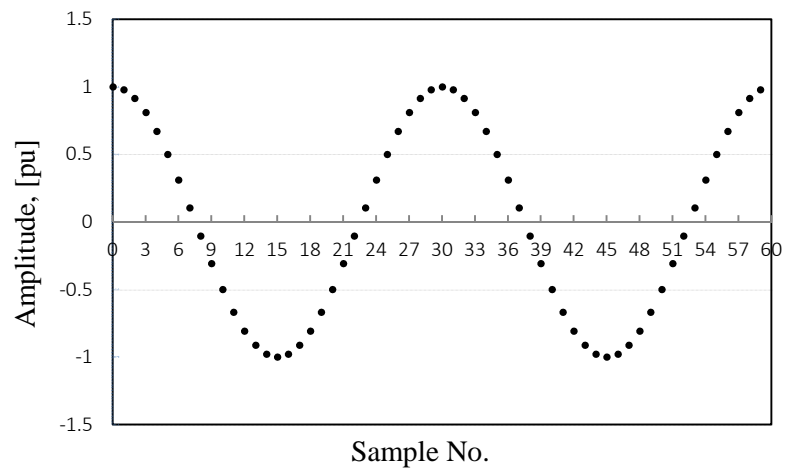


Figure 3.4 Generated point-on-wave synthetic input data for the model with non-zero ROCOF and ROCOA

As seen in the Figure 3.4 even though the changes are large (10% change in amplitude and increase by 3Hz of nominal frequency within a second), they are not obviously noticeable with the naked eye within one measurement window (2 nominal cycles). It is fair to assume that the values normally found on the power system, being smaller than the values here, would be even harder to observe visually.

3.3.2 Measurement method

To deal with the non-stationary signal generated, a nonlinear robust least squares fitting algorithm was selected, and MATLAB software used to implement the measurement (solving) concept.

The main thought behind the method used was that it minimizes the summed square residuals that are the difference between the estimated data point Y_i and the observed signal value y_i . Therefore, residuals are defined as

$$r_i = y_i - Y_i. \quad (24)$$

Then, the summed square of residuals is defined by

$$S = \sum_{i=1}^n r_i^2 = \sum_{i=1}^n (y_i - Y_i)^2. \quad (25)$$

Based on the fact that the input signal is nonlinear, the method must approach the solution iteratively [39] to lower the residual values.

Considering that real-world signals are noisy and there can occur sample “outliers” that would greatly impact the residual minimization process (when squared the outlier residual influence on the quality of the fit is amplified greatly) it is possible to reduce their effects or even remove them by using *bisquare* weights. Each residual is weighted according to its distance from the fitted line. Really extreme samples get zero weight [39].

The algorithm follows this procedure:

1. Start with a set of reasonable starting values. In normal operation, the values are the values at the end of a previous measurement window.
2. Calculate the Y_i values for the current set of input values.
3. Calculate a matrix of partial derivatives with respect to the values, ie. the Jacobian.
4. Weigh the residuals with the weighting algorithm.
5. Compute the weighted residuals. The residuals are given by

$$r_{wi} = \frac{r_i}{\sqrt{1 - h_i}} \quad (26)$$

where r_{wi} are the least-squares residuals and h_i are “leverages” that adjust the residuals.

6. Standardize the residuals:

$$u = \frac{r_w}{Ks}. \quad (27)$$

where K is a tuning constant and s is the “robust variance” given in the MATLAB documentation [39].

7. Calculate the weights as function of u . The bisquare weights are given by

$$w_i = \begin{cases} (1 - (u_i)^2)^2 & |u_i| < 1 \\ 0 & |u_i| \geq 1 \end{cases} \quad (28)$$

The final weight is the product of the two numbers produced by MATLAB, one called the “robust” weight and the “regression” weight.

8. Adjust the coefficients and determine whether the fit improves.
9. Iterate the process by returning to 2nd step until the fit reaches the specified convergence criteria [39].

This is one of the MATLABs default algorithms and it is used because coefficient constraints can be specified. It solves the nonlinear signal reasonably efficiently. Use of MATLAB also allows for code to be exported and re-used in C++ applications.

3.3.3 Output

The result of the algorithm is the set of all values in the defined mathematical model. Those are the values necessary to create a complete picture of the equation in the particular window of time. Once these values are obtained MATLAB offers additional metrics for the algorithm, like iteration count, that can be used for evaluation of the performance of the particular algorithm.

The output for the input signal generated in Excel spreadsheet is spot-on. It is clear that the estimation with clean signals works with precision of the computer. Declared values for the input signal (equation (22)) are:

- | | | |
|-------------------------------|-----------------|--------|
| - Amplitude | $X' = 1$ | [pu] |
| - Rate of change of amplitude | $C'_x = 0.1$ | [pu/s] |
| - Frequency | $\omega = 50$ | [Hz] |
| - Rate of change of frequency | $C'_\omega = 3$ | [Hz/s] |
| - Phase | $\varphi = 0$ | [rad] |

3.3.4 Goodness of Fit

Of particular interest is a parameter called Goodness of Fit (GoF). This is a number based on the residuals of the result of the measurement. In essence, a metric showing the quality of the fit is expected to be readily available for a fitting algorithm. For the purposes of the PMU measurement, such a metric offers something that measurements have not had available before: an estimate of the quality of each individual measurement made. This is entirely different than the typical statement of uncertainty that accompanies a statement of the result of a measurement, the statement

of uncertainty that is described in the Guide to the Expression of Uncertainty in Measurement [40].

Note that the use of GoF does not depend on the choice of measurement method. Once it is accepted that a representational measurement is an equivalent step to solving an equation, it follows that the results of any such measurement can be used to find the value of the residuals, and hence find a GoF metric. A GoF number can be used as a metric and calculated by any PMU. In fact, the application does not stop there and GoF can be used in other representationalist measurements (more information discussed in Annex 3) with different measurement methods (as long the observed quantity is available to compare to reconstructed mathematical model). This concept will be explored next in more detail [5].

For the test case described above, when the input signal is reconstructed with the values obtained by the estimation and is subtracted from input signal the residuals show clearly, (Figure 3.5) that the model and input signal are an almost perfect match.

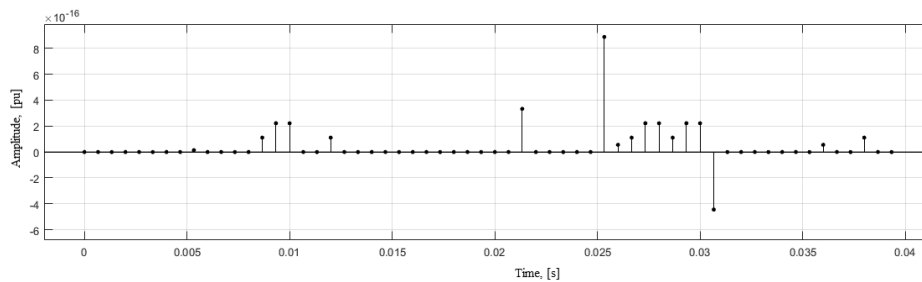


Figure 3.5 Residuals from reconstructed point-on-wave data subtraction from the input data

It comes as no surprise that the fit for a known mathematical model (a “clean” signal) should be this good, but this also shows that models can be adjusted, and the result can be improved. (Figure 3.6) shows how residuals look (larger by at least 10^{13}) if the mathematical model for fitting algorithm is just the phasor.

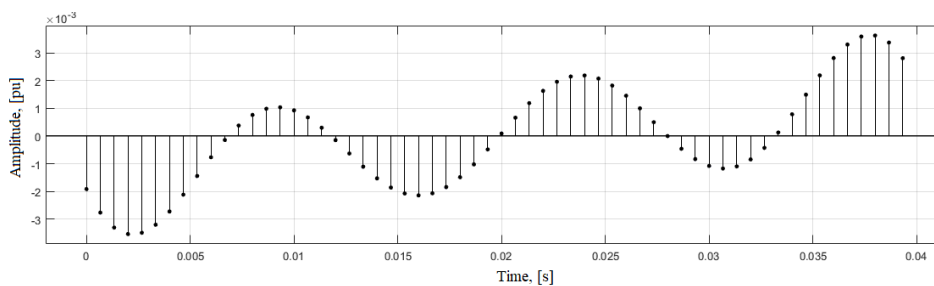


Figure 3.6 Residuals by subtracting reconstructed phasor point-on-wave data from the input data

In addition to variables in the equation the algorithm also can provide useful information about the fit, like for example already discussed residuals, R-square calculation, residual RMS calculation etc.

It was pointed out to the author that the fit refers to the signal and not to the parameters (e.g. it is possible to get a good fit with way too many parameters) and while

that is true, one has to go back to Rutman idea of model tractability and Carnap idea for real world transition into conceptual models. This is something that requires understanding of the physical properties being measured and the mathematical model of the measurement to draw the line where model is not tractable anymore and what level of real-world representation in the model is acceptable.

When the signal is not the “clean” signal seen above, the Goodness of Fit (GoF) shows itself to be a very useful tool coming out of the notion that the act of measurement is in fact solving of the equation. Once the measurement is done (made by fitting or not) the residuals enrich the system metadata – there is the original input signal, the method’s metadata, the mathematical model (equation), the declared values, and now a new parameter indicating the quality of the measurement process.

For an ideal synthetically generated perfect signals (yet non-stationary) it is clear that a perfect match can be achieved and that the residuals approach zero. In this situation all metadata and other parameters represent a non-existent perfect world that tells nothing about the real world.

The obvious answer for putting the method to the test is to try to estimate a signal that cannot be expressed in a single model (equation) for whole measurement window, like a step-change in phase of a sinusoidal signal. Visual representation of 180° step-change is given in the (Figure 3.7) and it is clear that the input signal cannot be described with phasor-like quantities. But for sure one can try and estimate the values (just like PMU has to for non-stationary signals). First, let us look at some synthetic signals that test the GoF method.

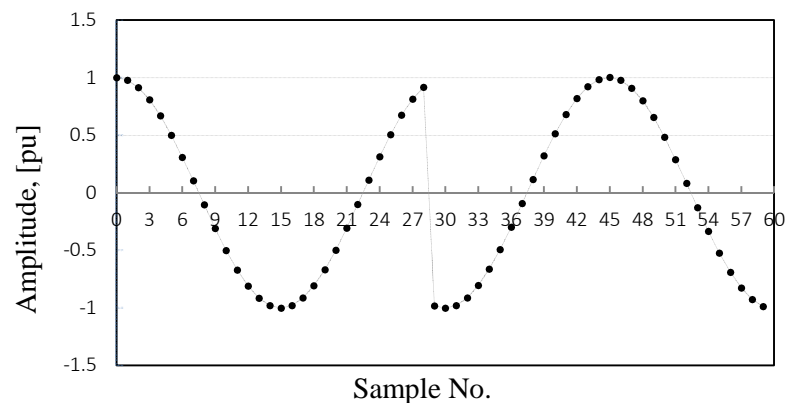


Figure 3.7 A 180 degree phase jump in the input signal

Consider the signal in the (Figure 3.7) with sudden change in phase by 180° . The estimation still can be made, and values can be obtained. In (Figure 3.8) there is the reconstructed signal from the declared values next to the input.

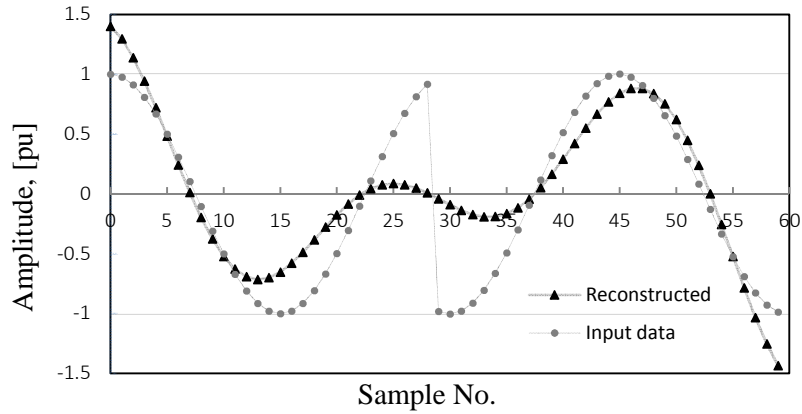


Figure 3.8 Input signal with step change in phase and its estimated signal

As stated in [7] there are two questions: what does user want to know, and what will the instrument tell him? The answer to the last one is clear for used estimation algorithm developed in MATLAB. The method reports the values for the reconstructed signal. But is this something that anybody wants to know? If the actual input signal is compared to the measurement values, it is arguably useless – the match is clearly not good. On the other hand, the result is “best” in the sense of being a least-squared-error estimate of the input using the model that is available. How “good” is that “best estimate”?

This returns the attention to GoF. With such indication it would be possible to declare the level of trust for the measurement. Rather than use the GoF as understood by MATLAB, a variation was created [5] in which the GoF is introduced as reciprocal value of the fit standard error normalized and expressed in decibels. The reciprocal has the advantage that the value increases as the fit improves, and the logarithmic compression of decibels keeps the numbers more accessible. The formula used was:

$$GoF = 20 \log \frac{X'}{\sqrt{\frac{1}{(N-m)} \sum_{k=1}^N (u_k - v_k)^2}}, \quad (29)$$

where N is the number of samples, m is the number of parameters being estimated in the equation, X' is the signal amplitude, u_k is the signal sample value and v_k is the estimated sample value. The parameter $(N-m)$ is called the residual degrees of freedom [41].

GoF calculated for the perfect signal is very good. In fact, it's down to precision of the computer at couple of hundreds of dB (for example for Figure 3.4 it is 304 dB). Where it really matters is describing measurements that don't fit and tell user how good or bad the measurement is at representing the real world.

Consider the signal in Figure 3.7. The calculated GoF value for this measurement is 7 dB which compared to 304 dB in Figure 3.4 is considerably less. This means that user confidence that the declared values really represents the reality should

greatly diminish. Further questions should be asked, like, what is going on in this particular measurement window? One information source is residuals. If plotted (Figure 3.9) they show interesting information.

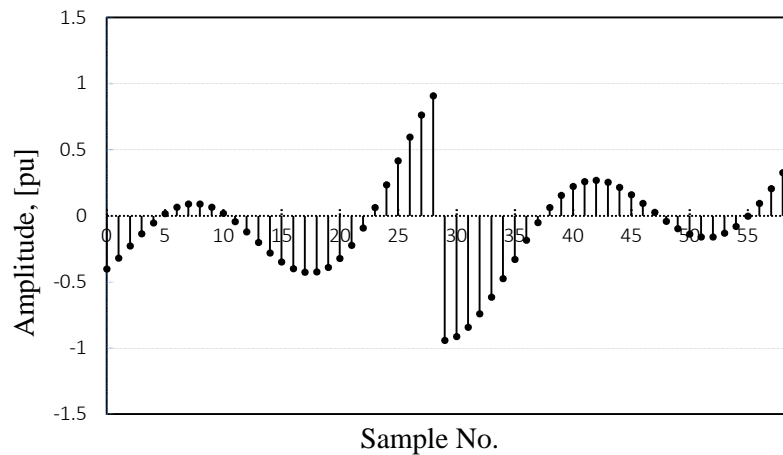


Figure 3.9 Residuals from estimated signal and input signal with 180 degree phase jump

It is evident that the algorithm must make a choice, to align to the first part of sinusoid or the second part. In both occasions declared values are not the ones for first half of signal or the second half, but the algorithm (PMU also) has to somehow find a reason for such signal behavior using the information that user gave to it (equation). In this case the best fit is if the signal is decreasing frequency very rapidly, to accommodate for the jump in phase.

Of course, the test signal in this example is somewhat extreme. Phase jumps do occur on the real power system (for example, when a phase-to-phase short circuit occurs) but at the location of a PMU it would be rare to see such a large step. In the following section, we will see some examples of how the goodness of fit responds with more realistic signals.

Parts of estimation algorithm are given in Annex 1. Estimation algorithm hereinafter in the text will be called SEMPR or “Signal Estimation by Minimizing Parameter Residuals”.

4 Analysis of the phasor-like model limitations

As the concept of phasor measurement is equivalent to an equation solving, it is necessary to understand the model limitations. Limitations in real world scenarios are posed from different sources, but probably the most prominent is the noise on the input signal. In order to get rid of it, PMUs use very heavy signal processing, including filtering. Filtering the signal has its drawbacks, like latency of the output (each measurement gets affected from previous measurements) and that is predominantly why during the testing for standard PMUs declared values over changing parameters are left out of evaluation [2].

In order to understand the limitations for the estimator algorithm it would be beneficial to use no filtering at all. In theory noise influence should be less than classical PMU because phase differentiation, which is very noise sensitive operation, is not implemented.

Another major benefit in this fitting method also would be completely independent measurements (no overlapping measurement windows, with no filtering adding “memory of an earlier signal”).

Noise in the power grid is very well known as a fact yet it is a very little understood process. There are many kinds of “noises”, like, harmonics, random noise, large disturbances etc. and some of them contribute most of the time. When signal is influenced by noise, this changes sample values and the measurement/estimation can contain error. This process may contribute to semantic coloration discussed earlier, but both of noise and distortion contribute to the error. It is important to note, that once the “noise” process is better understood and can be put in the model it no longer has influence on the estimation, because it is part of the equation.

4.1 Noise types and their effects

An empirical investigation was made of the effect of “noise” by adding controlled amounts to the basic quantity of interest, the sine-wave. For signal generation purposes there are different kinds of noise models available (usually called in names or colors), but for PMU model it only makes sense to use ones actually found in power system. Those are:

- harmonics;
- Gaussian white noise;
- Brownian noise (also known as *red noise* or *random walk*);
- DC offset.

Harmonics are defined as steady state distortions with frequencies that are multiples of the fundamental frequency. Based on Fourier series the power system signal with just harmonics can be expressed as sum of infinite number of oscillating functions [42] (phasors):

$$f(x) = \frac{1}{2}a_0 + \sum_{n=1}^{\infty} a_n \cos(n \omega t) + \sum_{n=1}^{\infty} b_n \sin(n \omega t) , \quad (30)$$

where $\frac{1}{2}a_0$ is the average amplitude value, a_n and b_n are amplitudes and n is the integer multiplier of the fundamental frequency. Harmonics occur as an effect from non-linear loads. In this case, non-linear loads, like inverters, consume non-sinusoidal current and this current (signal) contains harmonics that also influences voltage linearity and adds harmonics. Based on signal dispersion in Fourier series (30) and notion that the most expressed harmonics on the power grid are the odd number harmonics – 3rd, 5th and 7th harmonic (in 50 Hz system that is 150, 250, 350 Hz) [42] the signal distorted by harmonics can be easily obtained. Harmonics rarely exceed 5% of fundamental component amplitude, but for illustration purposes in Figure 4.1 showed 5th harmonic is 12% of fundamental.

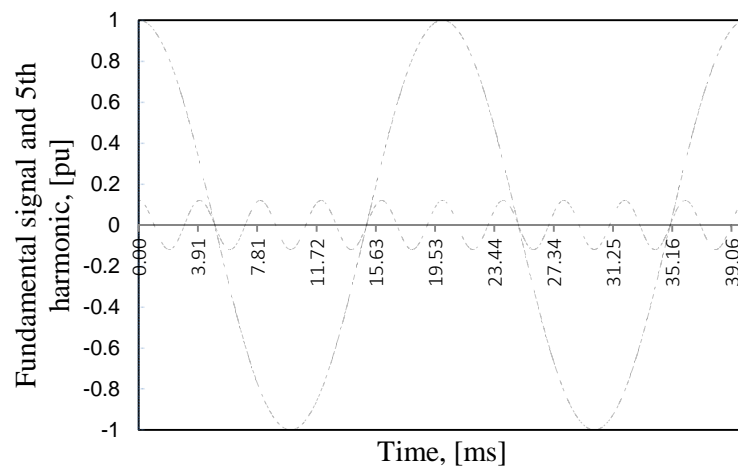


Figure 4.1 Fundamental frequency and 5th harmonic

Since the signals are additive all three mentioned harmonics can be added to the fundamental frequency (3rd; 5th and 7th harmonic with 20%; 12% and 8% pu). The signal is shown in Figure 4.2.

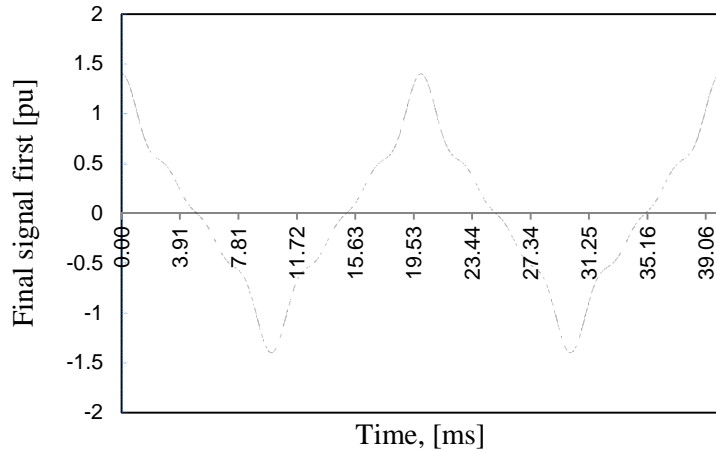


Figure 4.2 Harmonic distorted signal

As seen in picture the harmonics distort the sine wave to a point where it is far from textbook sinusoidal. This can be a problem for measurement algorithms in PMUs, because they expect sine wave at all times. This is why heavy filtering is applied to the input signal to get rid of harmonics. In SEMPR case however, it can be specified that the model contains harmonics and we can estimate them as non-stationary signals (harmonics will change because the fundamental frequency is never constant either). This will be investigated further.

The other noise type present in power grids is Gaussian white noise or normal distribution noise. The signature feature of this signal is its random nature and standard deviation. For this purpose, the noise signal was chosen with standard deviation of 0.5 and 3% amplitude and mean value of 0. For 50 000 samples the deviation is shown in Figure 4.3.

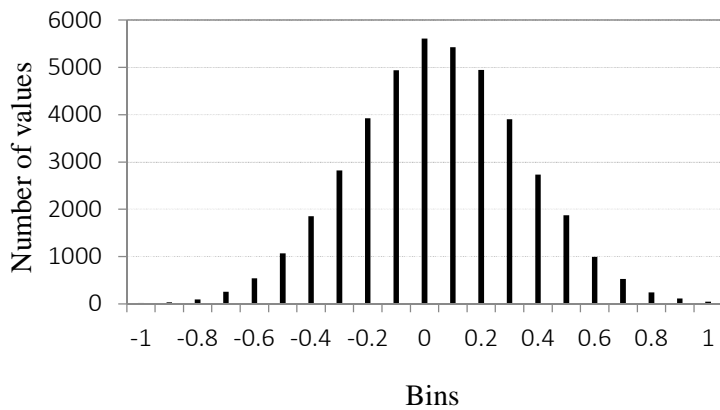


Figure 4.3 Normally distributed Gaussian white noise

When the noise is added to the harmonic distorted signal in Figure 4.2 the final signal is given in Figure 4.4.

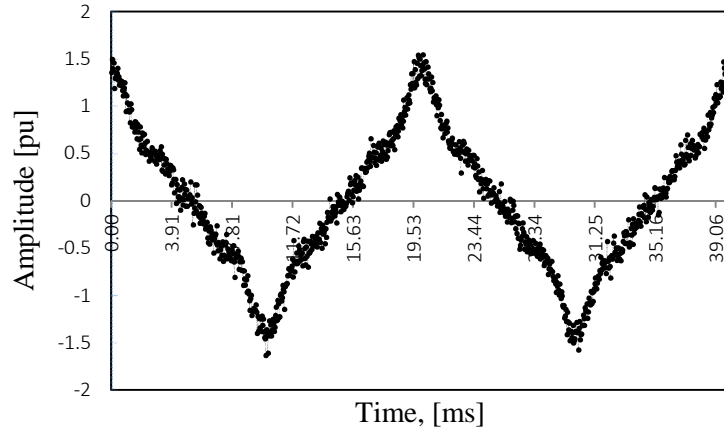


Figure 4.4 Distorted (noise plus harmonics) input signal

White Gaussian noise is used to simulate all kinds of random processes going on in the system and all systems nearby ranging from radio to cosmic background radiation. According to central limit theorem properly normalized random noise values tends to Gaussian distribution, as can be observed in Figure 4.3.

Brownian noise or Brownian motion (also known as *red noise* or *random walk*) is a very special kind of noise that is mostly associated with thermal and other stability issues of devices and measurement systems. Brownian noise can be expressed mathematically as integral of white noise. Given that ξ_t is a Gaussian random sample value with expected value $\mu=0$,

$$X_t = \xi_t \quad . \quad (31)$$

Then the Brownian motion value is given by,

$$X_t = \int_0^t \frac{d\xi(\tau)}{d\tau} d\tau \quad , \quad (32)$$

essentially

$$X_t = X_{t-1} + \xi_t \quad . \quad (33)$$

Brownian motion is usually caused by equipment or its parts beginning to decay and the parameters begin to drift away. This happens to clocks, reference values etc. This process usually is very tiny and very slow and that is why it influences every measurement window only slightly, but increasingly with time. Since for short time frames the Brownian motion is similar to white noise final input signal is similar to signal given in Figure 4.4.

Direct Current (DC) is also a very undesirable component of a modern AC distribution system. DC can be induced in AC network by failure of rectifiers and this adds unwanted current to other devices. DC current can overheat devices and saturate

transformers. DC can also be the result of a problem in the A/D converters in the PMU. The final test signal is given in Figure 4.5 with 10% pu DC offset.

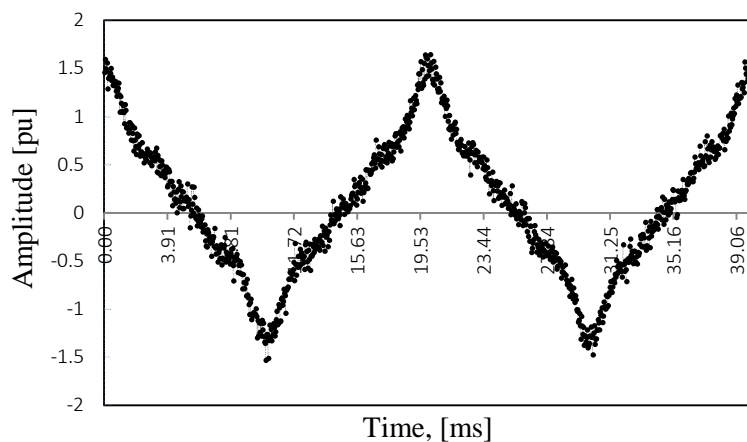


Figure 4.5 Distorted input signal

The final generated input signal consists of;

- Fundamental frequency of 50Hz and amplitude 1 pu;
- Harmonics: 3rd 5th and 7th with amplitude 0.2 0.12 and 0.08 pu;
- White Gaussian noise with 0.03 pu amplitude and mean value 0;
- DC offset with amplitude 0.1 pu.

4.2 Noise effect on the model

Considering the large disturbances given in Figure 4.5 it is clear that this wouldn't be typical situation in power system. By consulting AS "Sadales tīkls" and doing research on noise in distribution systems¹ more realistic values would be:

- 0-3 % harmonics;
- 0-1 % noise;
- 0-1 % DC offset.

SEMPR implements no filtering so all the disturbances have effect on the final declared value and estimation process itself. For the first understanding of the model and its properties handling distorted signal an additive disturbance is implemented. This means that every sampled noise value at the given moment in time is added to the input signal sample value. The true nature and mathematical models of the noise processes are still quite unknown. As in [17] "additive noise" to this model is a property we use to make the model tractable.

¹ Experimentally examined in Artis Riepnieks MSc. thesis "Vadāmības traucējumu noteikšana un izpēte zemsprieguma elektrotīklā viedajām mērīšanas sistēmām".

At first a small Gaussian white noise (0.1 %) is added to the 50Hz signal with amplitude 1 pu and ROCOF of 0.3 Hz/s. The sum of the signal and the noise is then fed into the SEMPR estimation algorithm.

Table 1

Estimated values of the input signal with 0.1% noise

Measurand	Input	Output
Amplitude, pu	1	1.00
Frequency, Hz	50	49.99
ROCOF, Hz/s	0.3	0.33
Phase offset, rad	0	5.00e-05

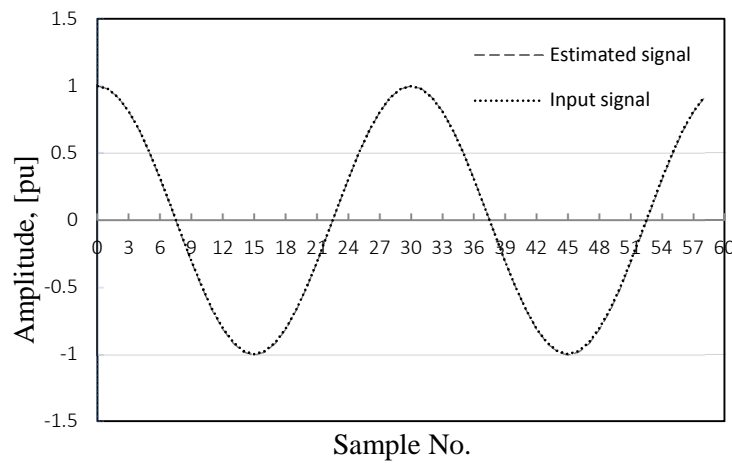


Figure 4.6 Reconstructed oscillography along with the signal estimate

As seen the Figure 4.6 the match is almost perfect. Even though the estimation is very close, the value difference is noticeable. When analyzing the residuals (Figure 4.7) it is clear that mostly residuals consist of the random noise signal.

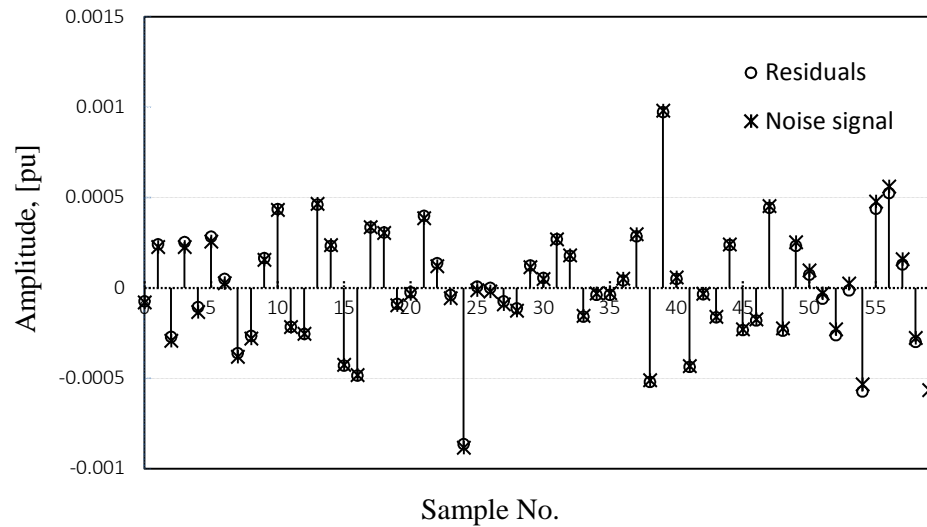


Figure 4.7 Residuals from estimation compared to the noise signal

The calculated error for this measurement is 1mHz in frequency and 30mHz/s for ROCOF estimation. This gives GoF value of 69.63 dB.

GoF is a good indication of the quality of the measurement e.g. 70dB would indicate that the model used can account at least for 99.999% of the real world observed. The GoF value decreases once the model cannot account for larger parts of the observed signal, like when phase jumps 180° or large part of the signal is noise/other disturbances. With GoF it is possible to evaluate each disturbance effects on SEMPR and chosen model (Table 2). As expected, by including the harmonics and the DC offset in the model, these “noises” do not prevent a good measurement. Gaussian and Brownian noise are not accounted for, however, and the fit is not so good.

Table 2

Estimated values of the input signal with different noises

Measurand model %	GoF, dB (Harmonics)				GoF, dB (Gaussian)				GoF, dB (Brownian)				GoF, dB (DC offset)			
	0.1	1	1.5	3	0.1	1	1.5	3	0.1	1	1.5	3	0.1	1	1.5	3
Phasor	61	41	37	31	68	49	46	40	37	17	14	8	59	40	36	30
Kirkham equation	61	41	37	31	69	49	46	40	37	18	14	8	59	39	36	30
Kirkham equation with harmonics, DC	304	318	310	307	69	49	45	39	51	29	20	8	264	233	231	246

By simulating different noise types at different amplitudes and using different models for measurement a couple of interesting conclusions can be observed by examining the GoF value summary given in *Table 2*.

- The Brownian noise impacts the measurement the most. It is understandable, as random walk increases with time;
- With lesser disturbance to a measurement is the Gaussian noise (the average value should be approaching zero), but since there is no mathematical model to predict noise values (random values) it affects all measurements equally.
- With small ROCOF (comparable to noise signal [4]) values the measurement quality is comparable with phasor model measurements, but one must keep in mind, that the small ROCOF values are what we are really after.
- Harmonics and dc offset can be described in the model and therefore improves the measurement for those types of disturbances. For Brownian noise the model assigns at least some of the random walk amplitude to dc offset so fit for “Kirkham equation with harmonics, DC” slightly improves.

Interestingly, a call for PMU noise performance levels is explained in [31].

4.3 Allan variance

SEMPR works exclusively in time domain so Allan variance, or *two sample variance* is appropriate way to measure the stability of the estimator in the time domain. Allan variance is widely used in precision clock and oscillator industry to measure clock stability due to noise, so the same principles can be applied to SEMPR stability while handling noisy signals. If the clock precision is dependent on oscillator stability and constant frequency of the oscillator in SEMPR method is depending on good and stable estimation of the system frequency. The Allan variance σ_y^2 as defined by David Allan is best shown in Figure 4.8.

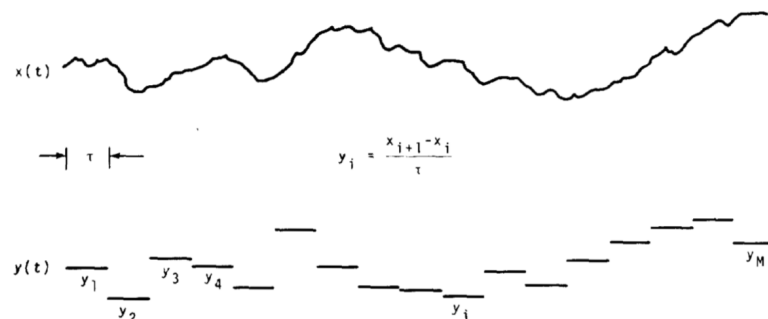


Figure 4.8 Measurements for Allan variance calculation [43]

Expressed mathematically in [44] and later in [45] as:

$$\sigma_y^2(\tau) = \frac{1}{2\tau^2} \langle (\Delta^2 x)^2 \rangle = \frac{1}{2} \langle (\Delta y)^2 \rangle \quad , \quad (34)$$

where the τ is the measurement interval and brackets $\langle \rangle$ denote ensemble average for infinite time. The essence of the variance is that the signal parameters are constant and taking three adjacent measurements x_n ; x_{n+1} and x_{n+2} spaced evenly by an interval τ . Averaged over measurement interval τ :

$$y_n = \frac{\Delta x_n}{\tau} \quad , \quad (35)$$

where Δx_n is the difference between the adjacent measurements $x_{n+1} - x_n$ as shown in Figure 4.8. Similarly, the average difference for the next two measurements can be written as

$$y_{n+1} = \frac{\Delta x_{n+1}}{\tau} \quad . \quad (36)$$

Now the change of the measurements between first measurement interval τ over to the second can be expressed by

$$\Delta y_n = y_{n+1} - y_n \quad . \quad (37)$$

This in [45] is called second difference (the difference of a difference) and indicated as Δ^2 (34). Allan variance is then computed over large strings of measurements and more measurements the better confidence on the estimate. Usually calculated Allan variance plotted as a function of measurement window length looks similar to Figure 4.9 [7]. Increasing measurement window gives smaller variances. If the noise process is Gaussian and the quantity being measured is a linear function, the slope of the line is -1 (i.e., 45 degrees). Doubling the time will halve the variance, but given long enough window lengths a minimum can be achieved after which the variance starts to increase. This is usually caused by drifting parameters or low frequency noise (like Brownian noise).

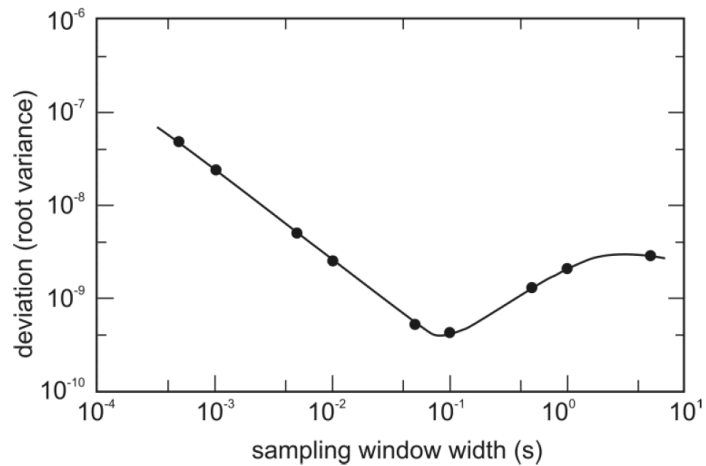


Figure 4.9 Deviation as a function of measurement length [7]

In PMU case, of course, the system is not constant. Even though the notion that the signal is constant during single measurement window, the next window the input parameters will have changed, and the fluctuations of parameters occurs naturally in power system.

The notion of constant parameters over the measurement window τ gives opportunity to use Allan variance for SEMPR frequency estimates (assumed constant through whole measurement window). Constant parameters are very doable with synthetic generated signals. This also allows to precisely control the noise parameters and estimate the limitations of the estimator in a sense of resilience to noise and different measurement window lengths τ .

Consider 1% white Gaussian additive amplitude noise on the input signal (22) with constant parameters for amplitude and apparent frequency. As shown in 3.3.3 with perfect signals SEMPR works flawlessly, but noise is adding imperfections on the input, therefore affecting the estimation and the output. Since the white noise has mean value of zero, given long enough, the average influence on the measurement should average to zero. By introducing 1% noise on the signal and using SEMPR the Allan variance can be calculated. Running the SEMPR on longer string of data (100 measurements), the 2-cycle measurement window gives GoF in range of 42-45dB. By making the frequency and amplitude estimation for the string of input data (1-50 seconds worth of data at 30 samples per cycle) with different measurement windows:

- Single cycle (0.02s)
- Double cycle (0.04s)
- 4 cycle (0.08s)
- 10 cycles (0.2s)
- 50 cycles (1s)

the Allan variance can be calculated for all measurement windows. The results are given in Figure 4.10 and Figure 4.11 where each dot represents **100** measurement variance at 1% additive white Gaussian noise.

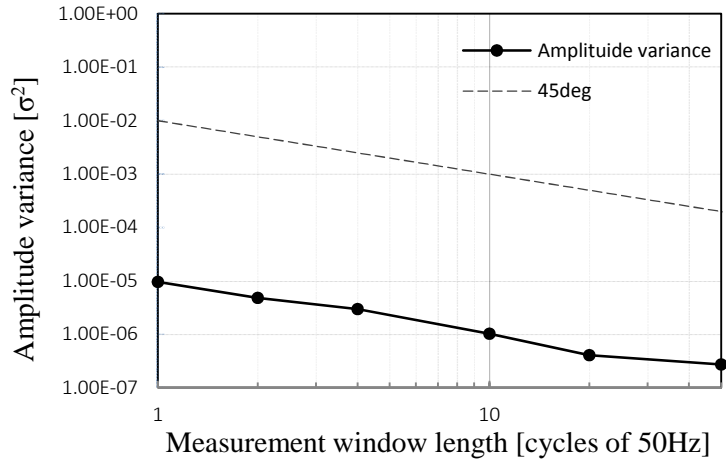


Figure 4.10 Allan variance for amplitude variable as a function of measurement window length

Figure 4.10 shows the measured variance of the amplitude parameter. The 45 degree Allan variance signature slope is added as dotted line to visualize the link between SEMPR measurement variance and simplest Allan variance. These slopes are the same.

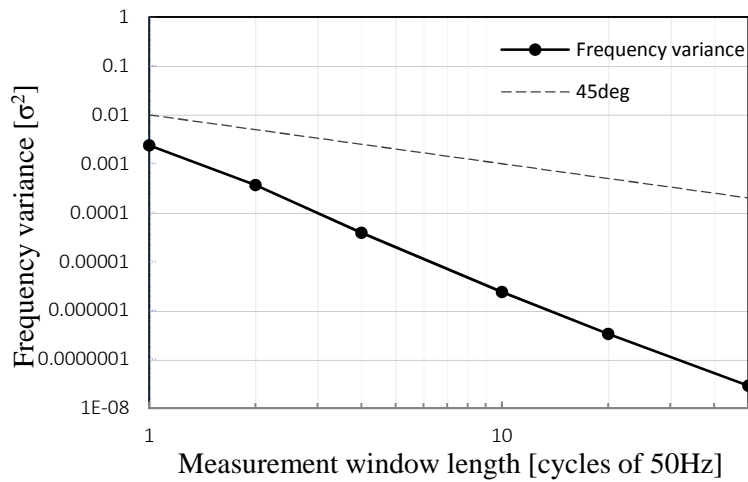


Figure 4.11 Allan variance for frequency variable as a function of measurement window length

Figure 4.11 shows the variance measured on the frequency parameter. It can be observed that given larger the measurement window the less the variance and more confidence in the measurement. This comes clearly from the definition of White Gaussian noise characteristics that over larger observation period the mean value approaches to 0 and does not affect the variance so much. It is also evident, that even though the variance is decreasing, it is not decreasing at the same rate as did the amplitude. Frequency is more sensitive to measurement window length and will benefit more from longer observation times (similarly like with zero-crossing counting method).

By adding larger amplitude noise, the variance would also change. Large information capacity of Allan variance plots gives opportunity to also show different inputs on a single graph. Different White Gaussian noise amplitudes are considered:

- 0.5%
- 1.5%
- 5%
- 15%

and added to the input signal. Then the Allan variance is calculated. The results for frequency and amplitude are given in Figure 4.12 and Figure 4.13.

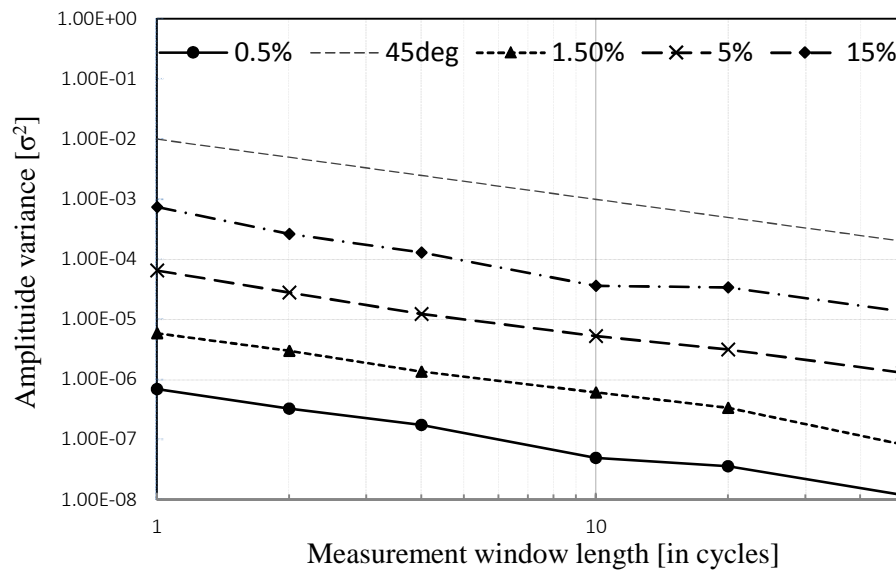


Figure 4.12 The Allan variance of the amplitude values as a function of measurement window length for different noise amplitudes

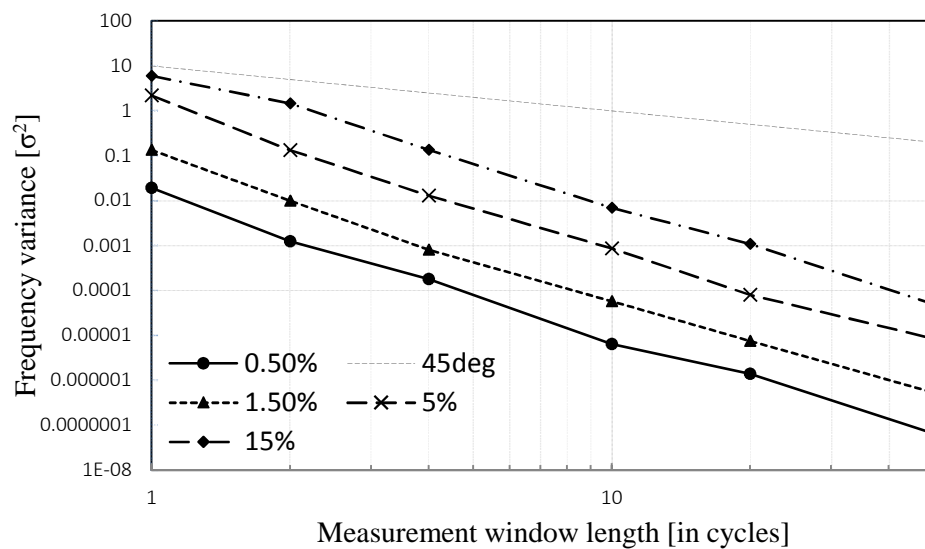


Figure 4.13 The Allan variance of the frequency values as a function of measurement window length for different noise amplitudes

Interestingly, independently from noise amplitude frequency estimate keeps the trend and confirms that the frequency estimation would greatly benefit from longer measurement windows.

Next, let's consider phase and ROCOF variances. The phase variance evidently follows the same pattern as the amplitude and tracks the 45-degree line.

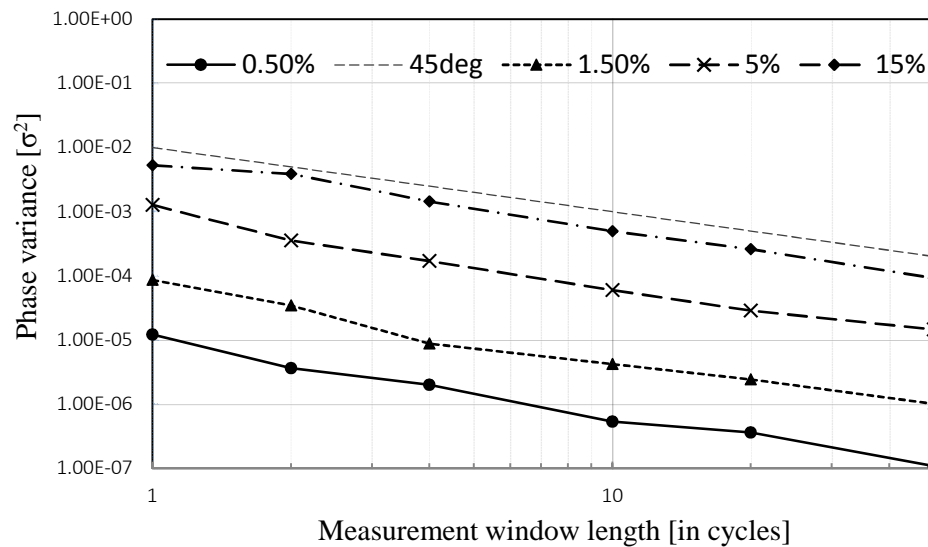


Figure 4.14 The Allan variance of the phase values as a function of measurement window length for different noise amplitudes

In power system case a parameter of particular interest is ROCOF. In the generated synthetic data, the ROCOF is set 0 Hz/s, but if the estimator is allowed to search for it, it is possible that there is a value assigned to ROCOF to better fit the model (this should be more pronounced in short-window cases). ROCOF value usually is very small and it gets drowned by noise very fast, so with assigned noise values for Gaussian white noise the estimates for short measurements should be unstable. ROCOF variance as function of measurement window length and with multiple level of noises is given in Figure 4.15.

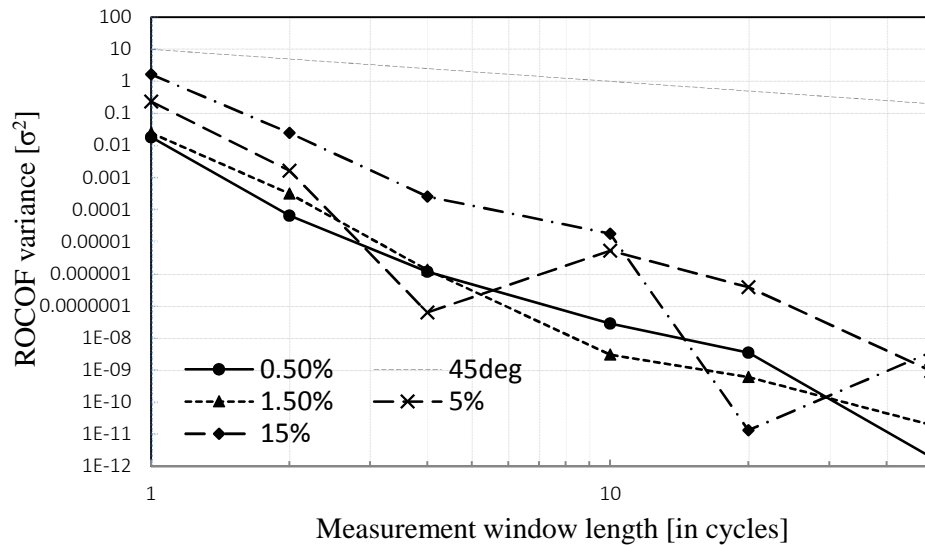


Figure 4.15 The Allan variance of the rate of change of frequency values as a function of measurement window length for different noise amplitudes

By the look of the Figure 4.15 it is clear that ROCOF benefits from longer observation windows even more than frequency measurement (no surprise here, as ROCOF can be thought of as frequency derivative). Short measurement windows produce widely variable ROCOF values, even if the ROCOF is constant. This poses the challenge to measure frequency and ROCOF at ever higher speeds and shorter windows. It is possible that ROCOF (whose contribution to the whole signal is about 5 magnitudes smaller than frequency variable [5]) for very short observation windows is not possible to measure in presence of even small noise (comparable to ROCOF itself). This concept may account for the fact that the IEEE Standard [27] was amended after a few years to become [1], with very “relaxed” requirements for ROCOF accuracy.

Overall, it is obvious that longer measurement windows produce measurements that are more reliable with low variance and higher confidence. The problem is that PMUs are asked to report the values within very short time (couple of cycles). Considering the measurement window length effect on measurement variance it could be possible to use different length measurement windows for different parameters since for a proof of concept the ROCOF measurement would benefit greatly from longer measurement windows.

So, the Allan variance clearly shows the benefits of having longer observation times, but how bad are the actual estimates? In Figure 4.16 all estimated values of frequency are shown for signal with 300mHz/s ROCOF and 5% added white Gaussian noise.

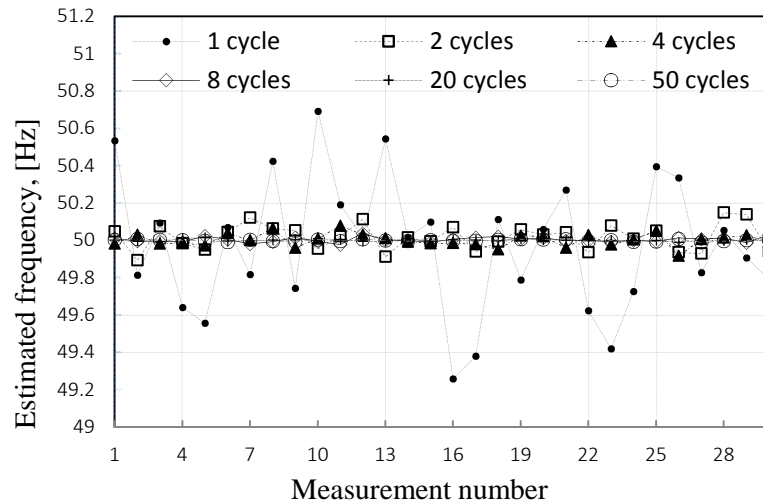


Figure 4.16 Estimated frequency with 5% added white Gaussian noise

It is shown that 1 cycle measurement variance is very large (from 49.2 Hz to 50.2 Hz) and larger measurement windows converge more to 50Hz. To better illustrate the variance of ROCOF in Figure 4.17 shows 50-cycle measurements.

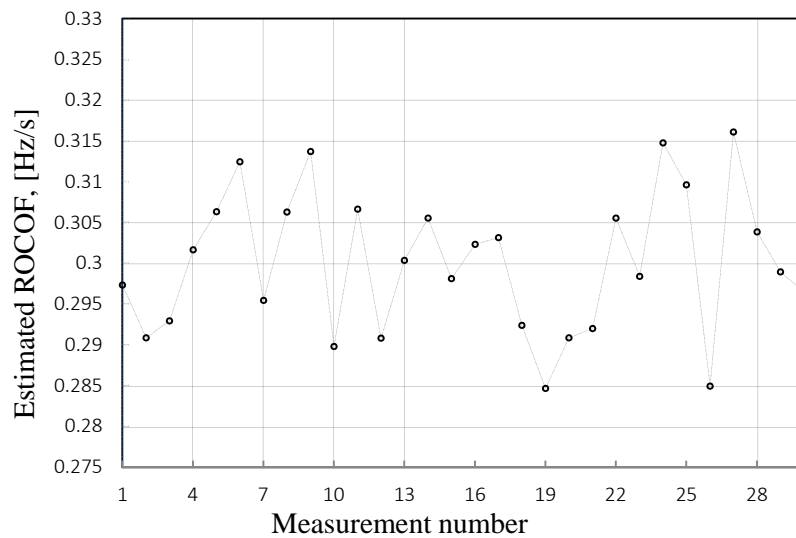


Figure 4.17 Estimated ROCOF with 5% added white Gaussian noise and measurement window of 50 cycles

In Figure 4.17 the variance for single cycle measurement is not very large also considering the difficulty distinguishing ROCOF from noise, but single cycle measurement variance showed up to 40Hz/s deviation, so 300mHz/s does not go on the same graph. It is very clear, that larger measurement windows reduces this variance quite drastically and for 50 cycle measurement windows the effect of white noise is reduced and the error is down to 15mHz/s max. Whether this value is realistic is not known, because the level of such noise in the power system is not generally known. It may be that this error level is actually pessimistic, and the measurement could be more accurate.

The other type of noise is low frequency Brownian motion or red noise. This noise will affect the Allan variance final part of the graph, since longer the measurement window, the larger the influence of this type of noise. Presumably a minimum can be found for variance to indicate the optimum window length for particular level and composition of noise. For Brownian noise, the amplitude levels are selected as:

- 0.009%;
- 0.03%;
- 0.5%;
- 1%,

for combined additive sample values with Gaussian white noise. Combined noise is then added to the input signal and fed into estimation algorithm. The same 100 measurements are made, and Allan variance is calculated. The results for phase estimation are given in Figure 4.18.

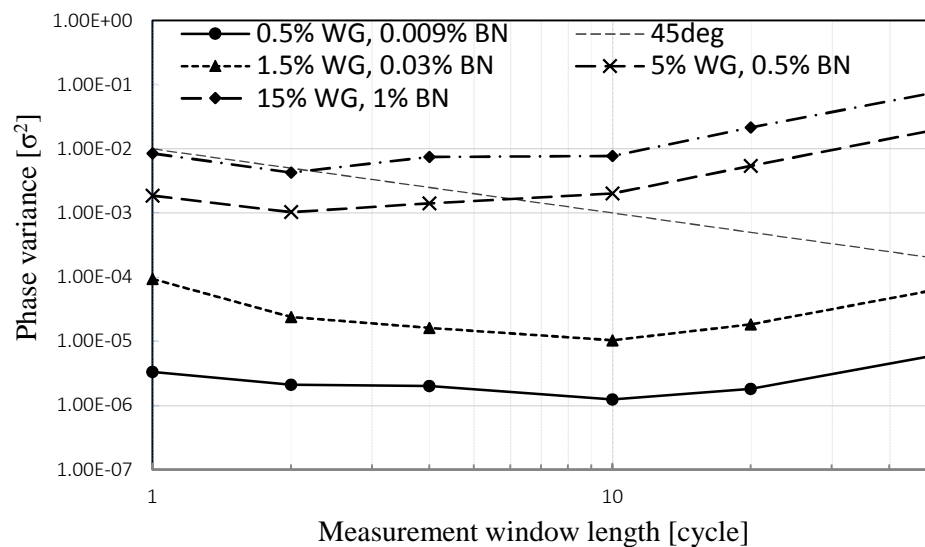


Figure 4.18 Allan variance of phase measurement affected by different levels of White Gaussian and Brownian noises as a function of window length

From Figure 4.18 it is evident that a minimum can be observed. With given resolution it appears that the optimum measurement window length for 0.5% White Gaussian and very small 0.009% Brownian motion is 10 cycles. Increasing or decreasing the window length from the optimum value will increase variance. For large noise value minimum variance is for 2 cycle-windows, but the variance is still 3 orders of magnitude larger just because of noise. This is mathematical calculation that could be performed in a PMU device as after measurement analysis and, since the point-on-wave sample data is available all model values can be re-estimated with different measurement windows, also different models.

On other hand, the noise might as well not be additive in its nature. The true processes of the noise characteristics are unknown and therefore very hard to put in mathematical models. In this case it was assumed that all noises are additive noise

values that were added to signal samples. It could be that the noise is affecting some parameters more than others, like for example, phase noise [30]. Rutman in [35] distinguishes between phase noise $\varphi(t)$ and amplitude noise $\zeta(t)$. It is not a coincidence that both noises have different symbols they are also different functions of time. This gives a lot of variation for signal generation and estimation. By adding different kind of noise to each parameter in Kirkham equation (22) it can be observed that the effects are different. With separately added 5% of white Gaussian noise to amplitude, frequency, ROCOF and phase it is shown that it affects the Allan variance on different parameters differently.

Figure 4.19 shows the change of estimated amplitude variation over increasing measurement window lengths and for different types of noises. The noise is added to each parameter in the Kirkham model separately so the effect on the parameter estimation is very different, as shown in graphs below.

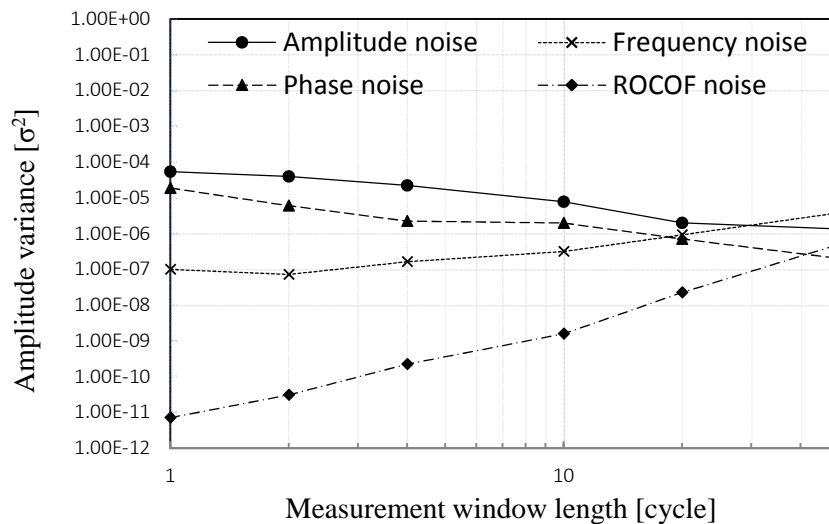


Figure 4.19 The change of amplitude estimation variance by different types of noises for differently sized measurement windows

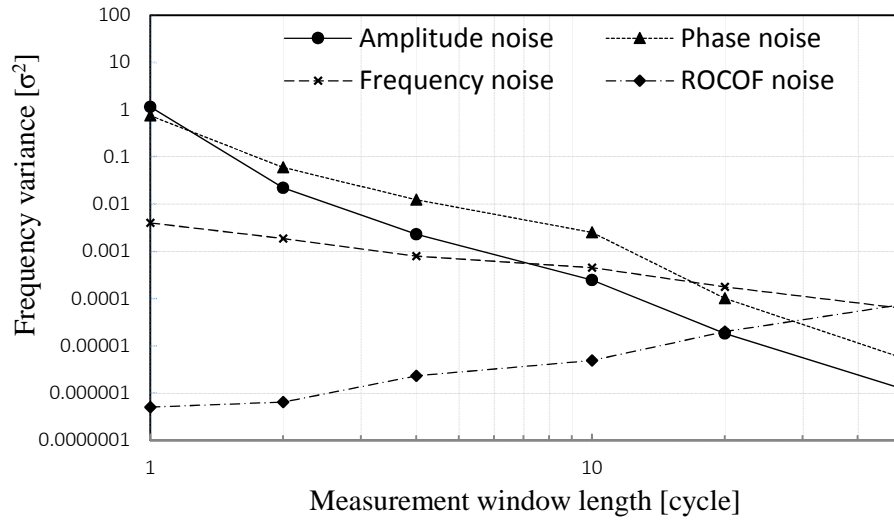


Figure 4.20 The change of frequency estimation variance by different types of noises for differently sized measurement windows

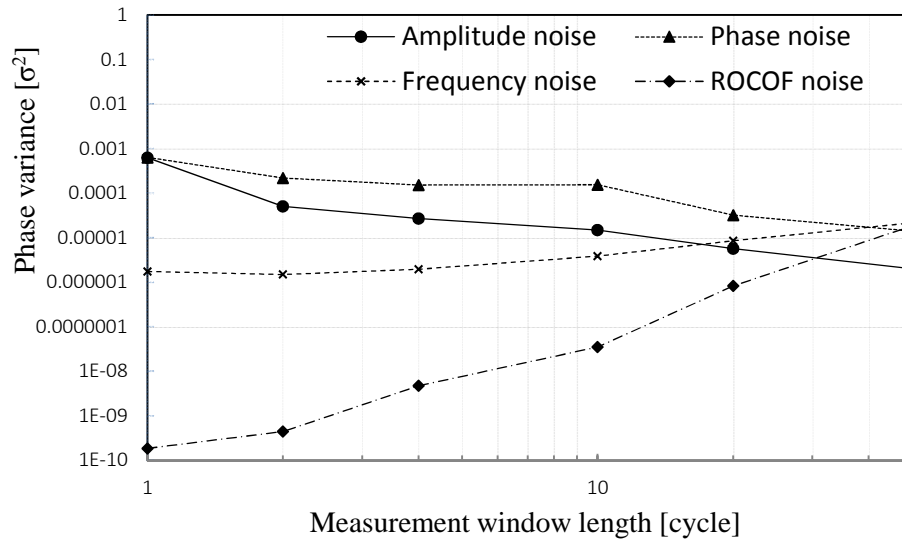


Figure 4.21 The change of phase estimation variance by different types of noises for differently sized measurement windows

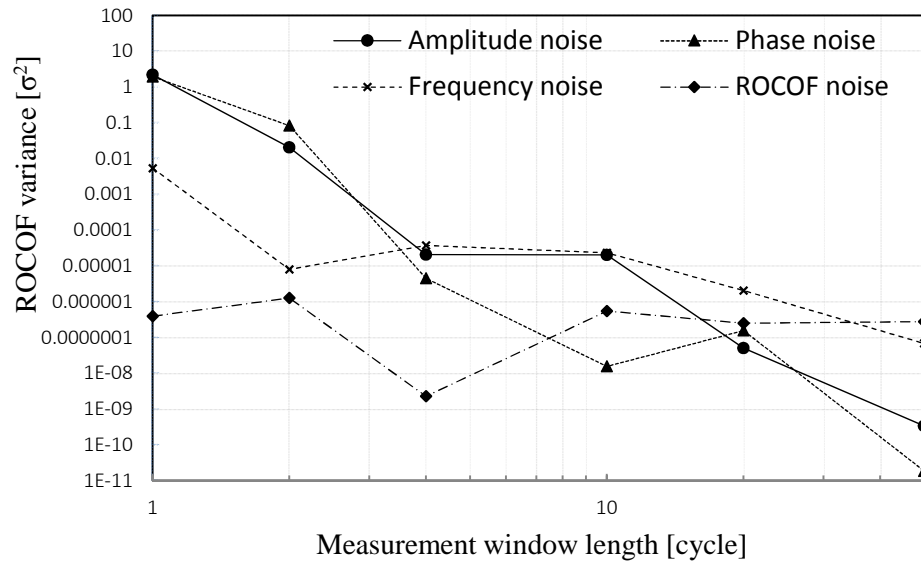


Figure 4.22 The change of ROCOF estimation variance by different types of noises for differently sized measurement windows

By observing Figure 4.19, Figure 4.20, Figure 4.21 and Figure 4.22 a couple of conclusions can be discussed:

- First of all, the ROCOF noise results in the smallest variance. This is due to the tiny ROCOF role in the model [4] and adding the noise it is still a tiny influence on the final result. However, estimation of ROCOF is very similar as estimation of noise signal and all variances for ROCOF are large for narrow window sizes;
- The most influential noises are the amplitude noise and phase noise. This is also the reason those are usually separated and examined as different functions. For phase estimation phase noise is the most influential, but for amplitude estimation the amplitude noise. This is not a huge surprise.
- Frequency noise theoretically cannot be distinguished from phase noise, but since it is a derivation of phase noise its influence is reduced below amplitude and phase noises;
- Interestingly some noises cause an increase in variance in larger observation windows. This is evident with frequency noise for amplitude and phase estimations. Also, ROCOF noise for longer measurement windows causes all parameter estimation variances to go up;
- Lastly, even though ROCOF noise influence on the variance is very small, it increases with observation time and by 1s it has reached the same influence on the estimated parameter variance as other noises. In Figure 4.19 it can be observed how all parameter variances from different noises become very close and the difference is within one order of magnitude. This makes 1 second observation a boundary where ROCOF and frequency noises could overwhelm amplitude and phase noises. So, for the lowest variance 1 s could become optimal because while with increasing

measurement windows amplitude and phase noise influence would decrease, frequency and ROCOF would increase, causing the same estimation variance.

4.4 Sampling variance

Advancements in device computing capabilities and digital technology over the last decades have made it easier than ever to implement faster and more capable microprocessors that can perform very fast sampling. This is the part of the work where we have to dig into sampling itself.

There are several “sampling theorems” for example the Fractional sampling theorem [46], the Walsh sampling theorem [47], the Zhu sampling theorem [48] and so on, just to mention few. The fact that there are so many related theories and topics points out the significance of signal processing to the modern technology for communication, control, and processing applications. However, all theories trace back to Harry Nyquist [49] and Claude Shannon [18].

Shannon’s theorem states:

If a function $f(t)$ contains no frequencies higher than W cps, it is completely determined by giving its ordinates at a series of points spaced $1/2W$ seconds apart. [50]

This means that if the signal $f(t)$ is band limited then it can be fully described by countably infinite set of values equally spaced by $1/2W$ seconds:

$$f(t) = \sum_{n=-\infty}^{\infty} \left(\frac{n}{2W}\right) \frac{\sin 2\pi W \left[t - \left(\frac{n}{2W}\right)\right]}{2\pi W \left[t - \left(\frac{n}{2W}\right)\right]}, \quad (38)$$

where n is the sample value obtained by sampling. Spectrum of such signal $f(t)$ outside band W is zero.

The main problem with real-world applications is that no real signal is perfectly band limited nor filtered to be perfectly band limited. In fact, in order for a signal not to have any energy outside finite frequency band, it must be infinite in time [51].

For real applications [52] suggests:

... Nyquist rate isn’t a line in the sand ... it is more like an electric fence or a hot poker; something what won’t hurt you if you keep your distance, but never something you want to saunter up to and lean against.

This something that designers of PMU systems have kept in mind knowingly or unknowingly, because each and every manufacturer chooses its own approach. In real devices the sampling rate can be from 24 samples to 512 samples per cycle. This raises the question – are we doing oversampling in PMUs? Sampling rate nowadays is something that can be changed by a software (firmware) change, so it is very doable. What then would be the optimum sampling rate? In theory it can be deducible with measurements and their variance.

In 1968 Karl Johan Åström in [53] discussed different sampling rates or time analysis of N samples at equal spacing h . He shows how there is an optimum choice of h , an optimum value to keep the variance down. By considering a stochastic differential equation:

$$dx = -\alpha x dt + dw \quad , \quad (39)$$

where α is a parameter to be estimated, $\{w(t)\}$ is random walk (Wiener process) and values x are observed at sampling intervals with equal spacing h . It is then mathematically shown that the smallest variance is given by

$$\text{Var } \hat{\alpha} = \frac{\alpha^2}{N} f(\alpha h), \quad (40)$$

where

$$f(x) = \frac{e^{2x} - 1}{x^2}. \quad (41)$$

The graph of the function given in Figure 4.23 shows that there is a minimum for the variance of α estimate given by

$$\hat{\alpha} = 6.177 \frac{\alpha^2}{N}. \quad (42)$$

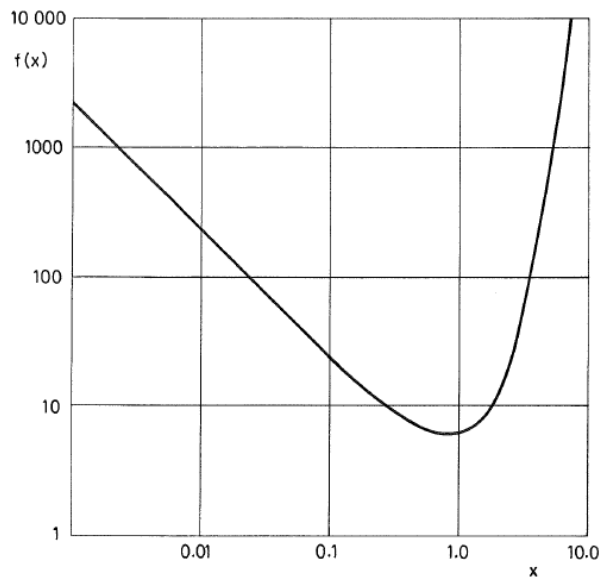


Figure 4.23 Graph of the function $f(x) = (e^{2x} - 1)x^{-2}$. The variance of the estimate $\hat{\alpha}$ using N values with the spacing h is $\alpha^2 f(\alpha h)/N$. [53]

The conclusion given in [53] for optimum sampling choice is $h = 0.797/\alpha$ which gives the smallest variance of $\hat{\alpha}$. The variance of $\hat{\alpha}$ increases significantly for sampling rates lower than h (larger sampling intervals).

Considering the practical implementation of SEMPR it should be also possible to determine the optimum sampling frequency based on the components (harmonics and noise, not only Wiener process) in the signal. In such case the optimum for the sampling rate would also be very well described by a variance value, but instead of changing observation time, one would change sampling rate. It should be possible to determine the optimum experimentally by implementing SEMPR. Sampling variance then can be expressed similarly to Allan variance, but instead averaging the measurements over increasing time period, we can average measurement over increasing sample number, but keep measurement window the same.

Input signal similar to one described in Section 4.3 was used to determine the optimum sampling frequency for noisy input signal. Since with clean synthetic signals SEMPR works flawlessly even with few samples, the minimum is set at this value, but maximum at fastest known commercial application in micro-PMU at 512 samples per nominal cycle [29]. Every dot in Figure 4.24 represents the variance for 50 measurements.

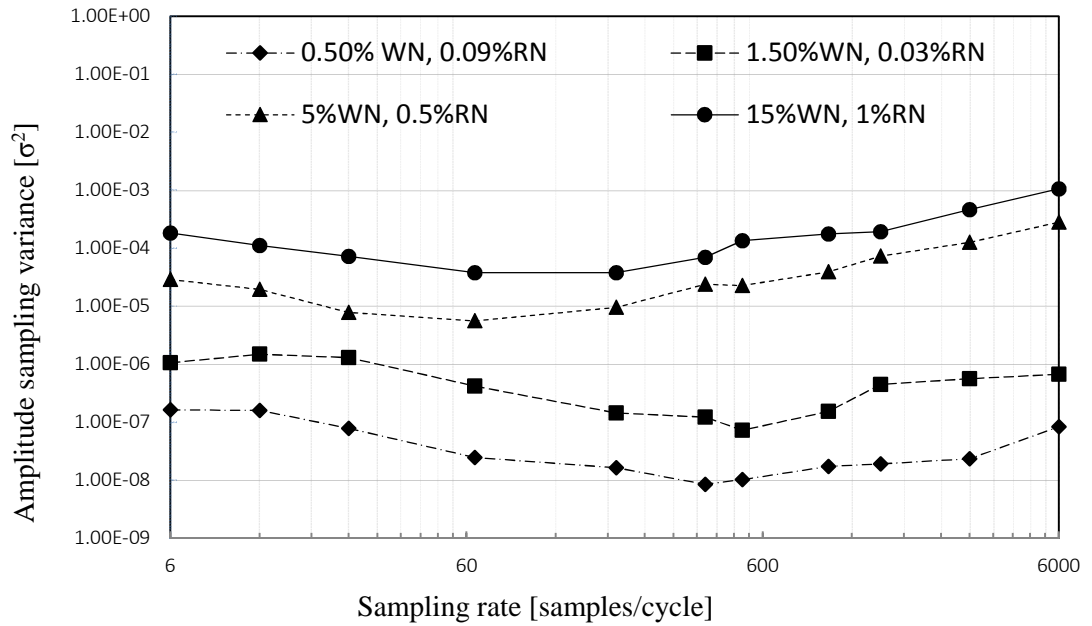


Figure 4.24 Sampling rate variance for Amplitude estimation

The simulation results in Figure 4.24 shows an interesting trend, that includes a minimum condition for variance. Of course, the smallest variance is for smallest of noises, but three other interesting observations can be made:

- The optimal sampling frequency decreases with larger noise influence.
- With fairly plausible noise levels (0-3%) the optimum sampling frequency is in fact somewhere between 192 and 512 samples per cycle (in this simulation closes point is 384 samples per cycle). This is in a same category as for micro-PMU, therefore their sampling frequency could be around optimum.
- The curves are all relatively flat, implying that a change in sampling rate of a factor of five or perhaps even ten would likely not make a significant change to the measured results.

This also shows that gross under-sampling and over-sampling should be avoided and by purely mathematic calculations it is possible to find an optimum sampling frequency based on the typical signal that the device should be observing.

5 Experimental data analysis

During the research in United States of America the real-world point on wave data was shared from AEP (American Electric Power) power network. Unfortunately, all attempts to get similar data from Latvian transmission system operator AST (AS “Augstsprieguma tīkls”) was unsuccessful as they were met by silence. Therefore, with permission from AEP anonymized real data analysis was done with available EHV (345kV 60Hz) system data.

The data obtained were samples, taken at 3.840 kHz sampling frequency (64 samples per cycle) and lasting about a second. Data includes 3 phase voltages before and during a fault in a 345kV line with line-to-ground fault along with multiple cycles of system recovery. This sequence allows us to compare real PMU measurements to SEMPR during nominal operation, fault, and system recovery.

Happenings during fault is of a particular interest and the reconstructed waveform can be observed in picture. It is clear that fault happens on 59th sample of the two-cycle measurement window. It looks that fault is most pronounced in phase C and perhaps phase A, but the data do not suggest a solid short circuit. Perhaps it represents contact with a tree, or a distant fault. Probably the most important observation is that the signal after fault does not resemble sine wave, yet PMU has nothing else to report – just sine wave parameters. Notice that the amplitude for the second cycle of measurement window in phase C is significantly low and SEMPR should be able to accommodate for that with ROCOA (Rate of change of amplitude). During the Fault in phase C the fault current exceeds 500A.

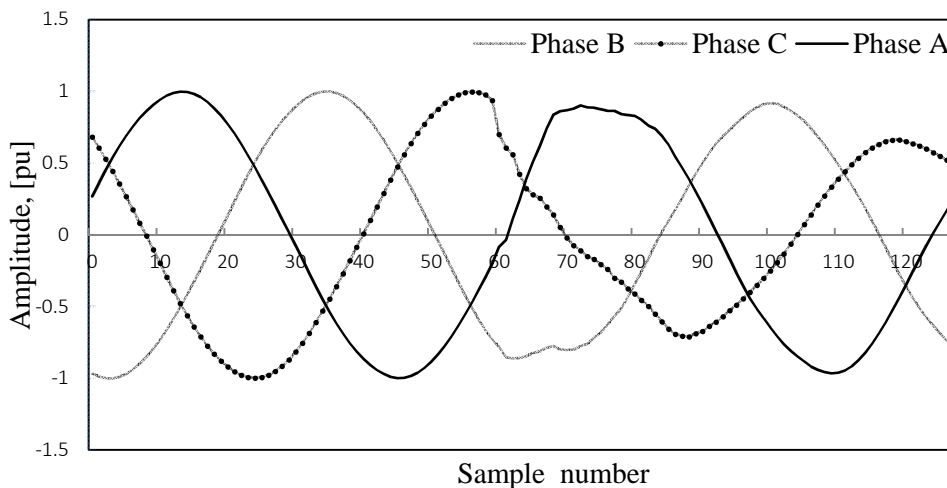


Figure 5.1 Fault in 345kV EHV three phase system

The data is accompanied with reported phasor values of the industrial PMUs so the GoF can be calculated and PMU performance can be determined. Couple cycles prior to fault PMU reported values for phase C phasor are 0.990 pu amplitude, 44.289^o phase, 60.000 Hz for frequency. Using these values it is possible to reconstruct the

signal that PMU has reported and compare it to the real oscillography. The result is given in the Figure 5.2.

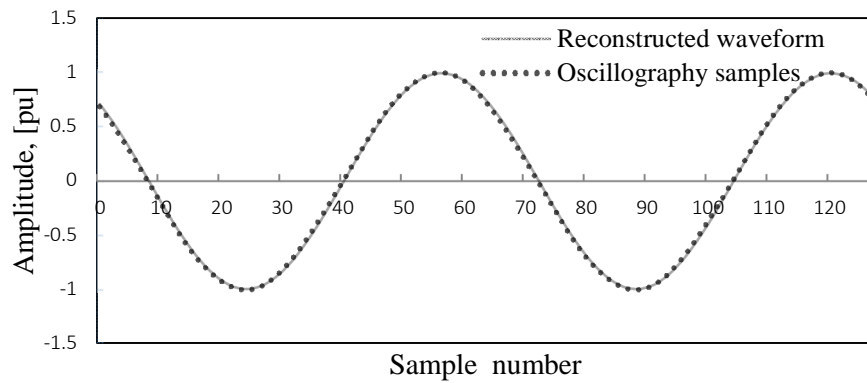


Figure 5.2 PMU reconstructed signal comparison with observed oscillography data

The match between two lines is very good, indicating that PMU values correctly represent situation in the system. This goodness of fit, as we discussed earlier, can be put in numbers from the calculated residuals, given in picture Figure 5.3.

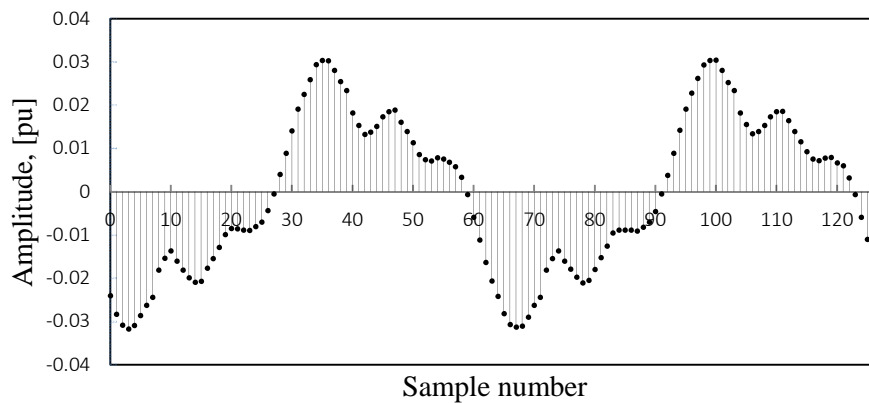


Figure 5.3 Residuals for PMU reconstructed signal and observed oscillography

The GoF level for this measurement is 34.88 dB and from Figure 5.3 it can be observed that the real signal contains large fundamental component as well as some periodic higher frequency components that PMU doesn't account for. Residual peak values are around 0.03 pu or 3% of the fundamental.

When similar task is performed to 1 second worth of data the picture of GoF is given in Figure 5.4. Plotted along GoF values are the current values to indicate fault duration.

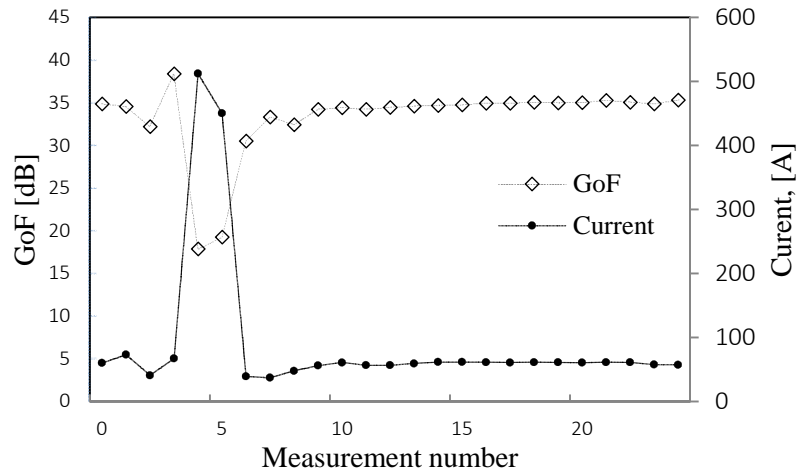


Figure 5.4 Goodness of Fit for 60 measurements with corresponding current measurements for phase C

It is clear that during fault the GoF values decrease significantly (approximately 20dB) and current increase corresponds well with obtained measurements. The GoF indicates that the wave is no longer sinusoidal in shape (PMU can no longer describe well the signal Figure 5.1) and can be provided along the reported values in real time.

Note that the GoF values during normal operation is more or less consistent and residual values are also. This indicates a constant slight mismatch in phase. The effect seems to be caused by the harmonics that are present in the signal.

When we zoom in on what is in Figure 5.4 measurement No.4 PMU signal reconstruction show exactly what is asked of a PMU – cosine wave, even if it is not the best representation of reality (Figure 5.5). Also note that the effects of the fault are present at least for 4 cycles (two measurement window lengths). Fault effects over 4 cycles given in Figure 5.6 with significant drop in voltage and recovery overshoot at the peak of 4th cycle.

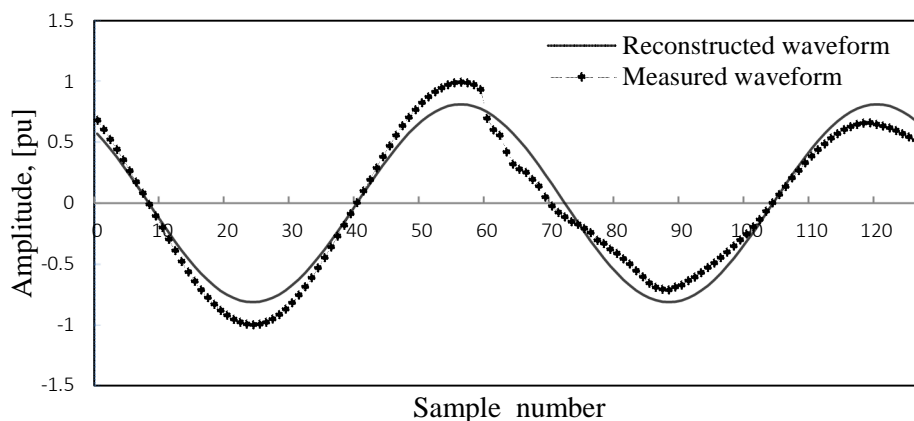


Figure 5.5 PMU reconstructed signal comparison with observed oscillography data during fault in phase C

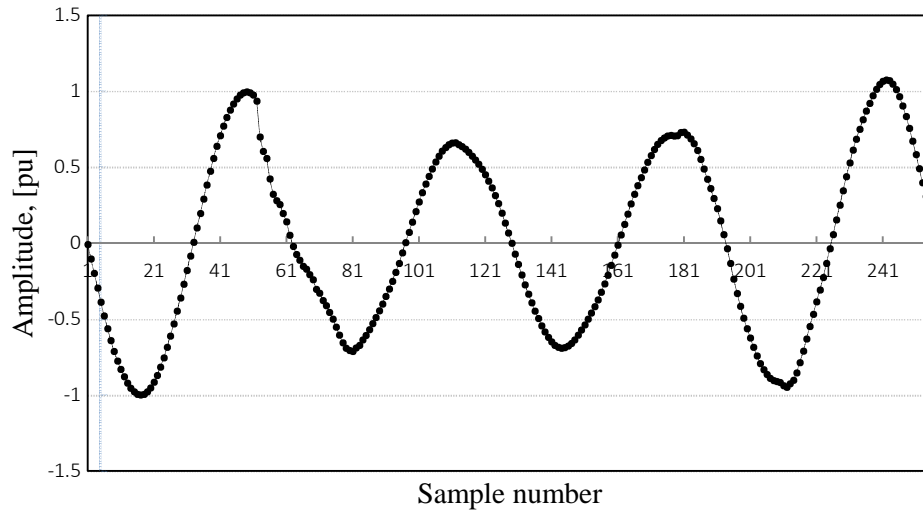


Figure 5.6 Fault in EHV system phase C, over 4 nominal cycles

The values reported by PMU are 0.803 for amplitude and 59.961 for frequency. It is clear that this representation by a phasor in this case doesn't work well, and the GoF is only 17 dB. In Figure 5.5 and Figure 5.6 no peak value is the same, though PMU has to report a single value and that is clearly not a good match to the observed signal as no peak value matches 0.803 pu.

5.1 Real data estimation vs the models

The phasor measurement unit was created to measure power system parameters, on the assumption that the system could be well-represented by a phasor. That means almost steady-state. The system is far from this condition during a fault. A commercial PMU includes much filtering in its design, and its response to a fault would be largely determined by the characteristics of the filters. SEMPR, on the other hand, includes no filters, but is (like the commercial PMU) trying to fit a phasor to a non-phasor signal.

SEMPR therefore gives as its declared values the least-squares best fit of a phasor to the distorted signal. A commercial PMU will give some other estimate based on its filters. Neither is “right,” because both assume a phasor model. Whether the output of either method is useful would depend on the purpose intended for the result.

Next, I explored the possibility of modifying the SEMPR model for this real-world signal estimation. The main advantage of SEMPR is that the model is selectable freely, so different models can be applied (also with capabilities to run them simultaneously as parallel processes). At least 3 models are worth looking at:

- Phasor model (6);
- Kirkham model (23);
- Kirkham model with ROCOA (22).

All measurements are performed with the same 2-cycle measurement windows and the same 1 second real-world input data (phase C). The result compilation is given in Figure 5.7.

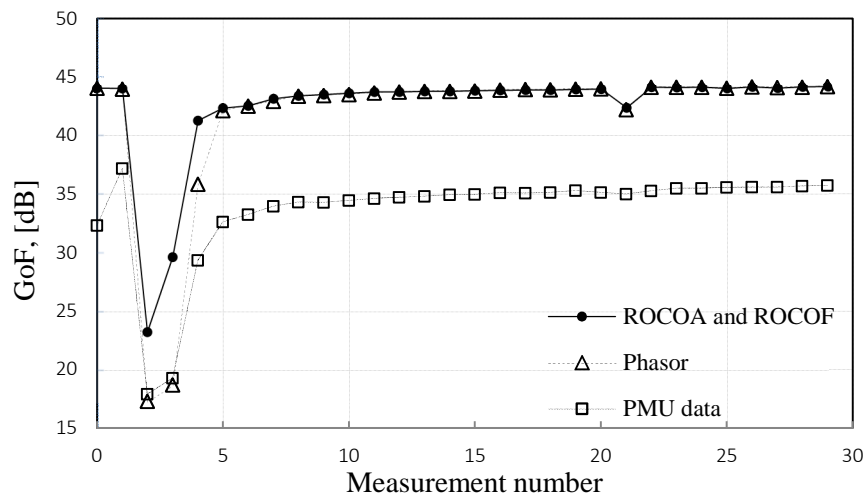


Figure 5.7 GoF calculation for SEMPR measurements compared to GoF calculations from commercial PMU declared values

It is clear that in this SEMPR can achieve better signal representation, especially during fault conditions. Over nominal operation SEMPR produces results on average 8 dB better than PMU values, but over fault there is 11dB difference. Interestingly there is not a lot of difference between SEMPR with ROCOF/ROCOA and simple phasor model during normal operation. This indicates that over nominal conditions PMU also has very good representation of the real world. It is also worth noting that during fault conditions SEMPR with phasor model is no better than PMU in making sense of non-sinusoidal wave, therefore the key is not in the method, but in the model.

Interestingly measurement No.21 (Figure 5.7) indicates slight drop in GoF from SEMPR measurements and very slight worsening of GoF in PMU declared values. This shows that SEMPR (independent 2-cycle measurements) is more sensitive to change of conditions and PMU could roll-through some very minor and fast changes in input signal due to signal filtering and latency. This is also indicated by the recovery speed of GoF after fault, where SEMPR shows very rapid recovery (measurement No.5) but PMU is slower to react.

Broadly speaking, one might say that none of the measurements gives a good match to the faulted signal, and all give a better match before and after. If the purpose of the measurement is to know the cosine parameters during the fault, none give much hope. On the other hand, if the purpose is to know that something has caused the signal to go non-sinusoidal, all methods are roughly equal. Some differences are explored next.

Estimated values during fault (measurement No.3) is 1.072 pu for amplitude, -28.848 pu/s for ROCOA, 60.639 Hz for frequency, -33.727 Hz/s for ROCOF, and

46.071⁰ for phase. This means that for amplitude SEMPR estimates that the voltage is dropping by astonishing 28 pu per second, or 0.23 pu per cycle. This means that in one cycle voltage level is estimated to decrease by at least 81kV. ROCOF value also indicates slowing down of the sine-wave by 33 Hz per second.

When plotted together the results of SEMPR shows clearly better fit (Figure 5.8)

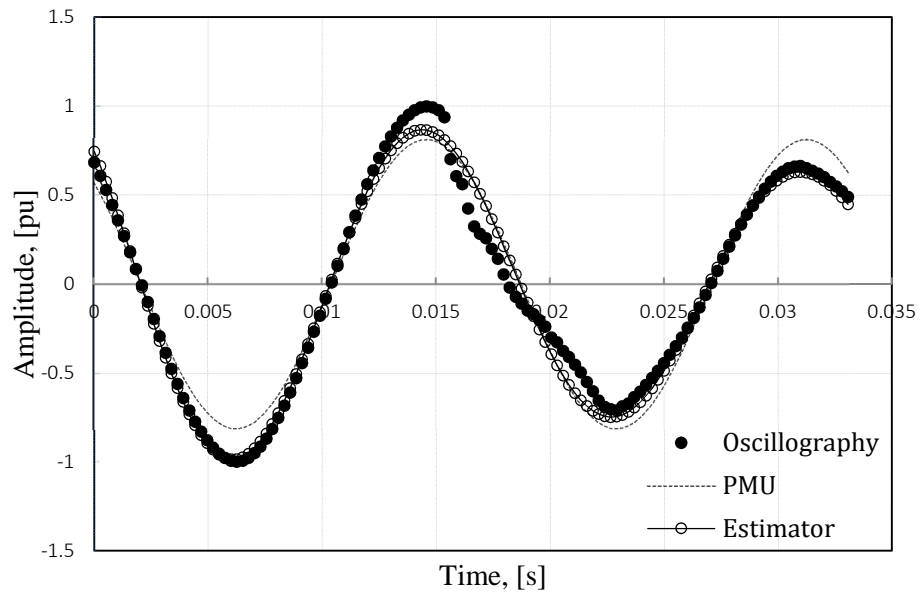


Figure 5.8 SEMPR algorithm reconstruction along with PMU reconstruction and real oscillography data

It is evident that SEMPR makes better estimation of the signal and for large parts of input data the estimation and oscillography lines are indistinguishable while PMU data reconstruction underestimates the peak values in first half of the measurements and overshoots at the second. It is made more visible if we look at the residuals in Figure 5.9.

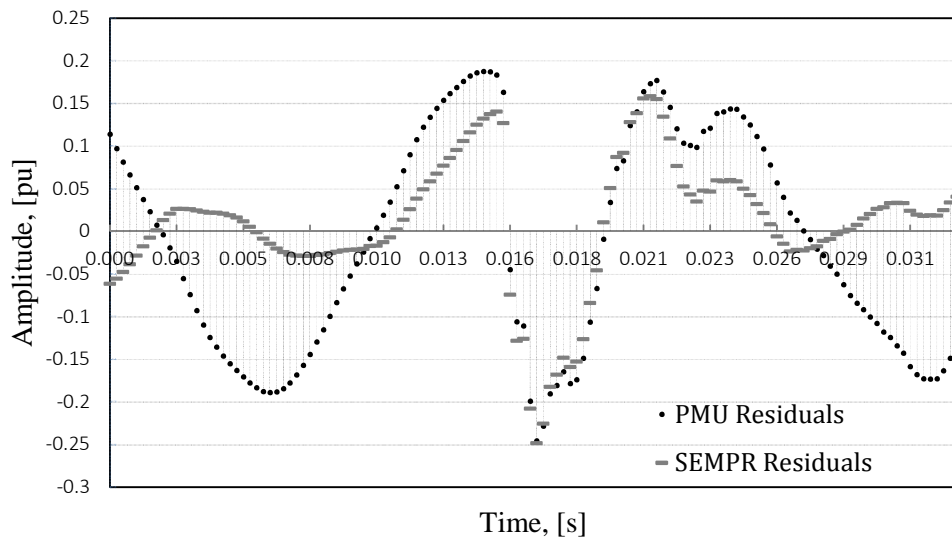


Figure 5.9 SEMPR and PMU measurement residuals during fault measurement

It is shown in Figure 5.9 that the residuals during the actual fault are almost equally large showing that both models don't represent the fault conditions fully, but right before and after the fault SEMPR shows much better results than PMU calculated residuals. It shows that it is beneficial to allow the model for more degrees of freedom and give the observer more tools to describe the signal e.g. allow the amplitude and frequency to change within the measurement window.

5.2 Real data variance analysis

Consider the same AEP data used for fault measurement analysis. The fault occurs at the beginning of almost one second worth of sample set. A PMU looks at the fault in two cycle measurement windows, but SEMPR can look at it even at half-cycle windows and 4 cycle windows (using model of a phasor). The frequency figures are given below.

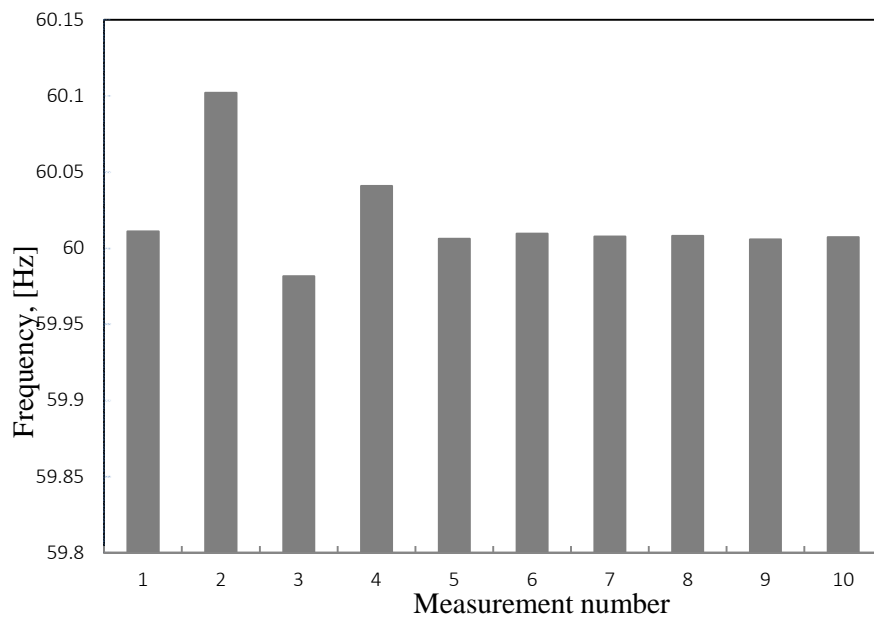


Figure 5.10 4-cycle measurement window measurements for data including EHV line fault

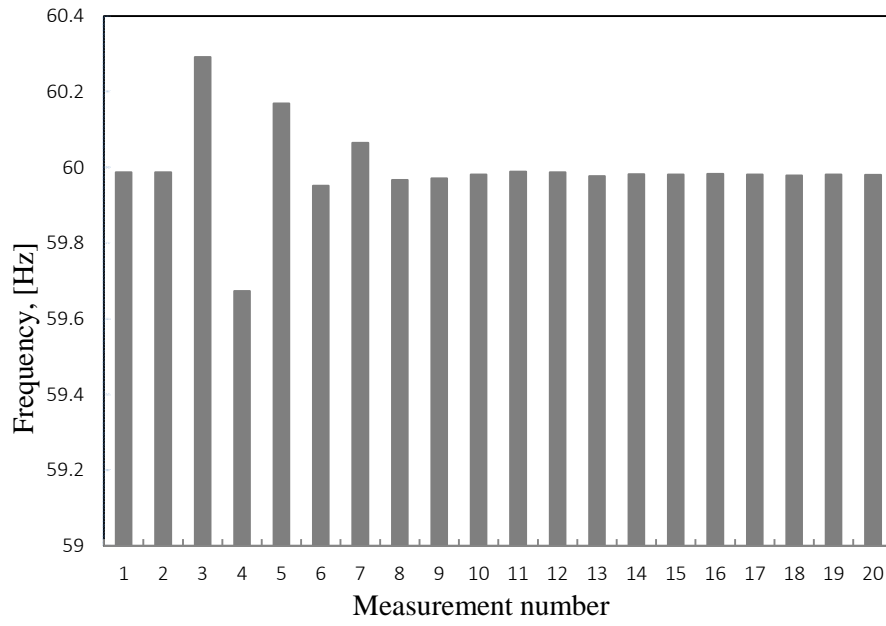


Figure 5.11 2-cycle measurement window measurements for data including EHV line fault

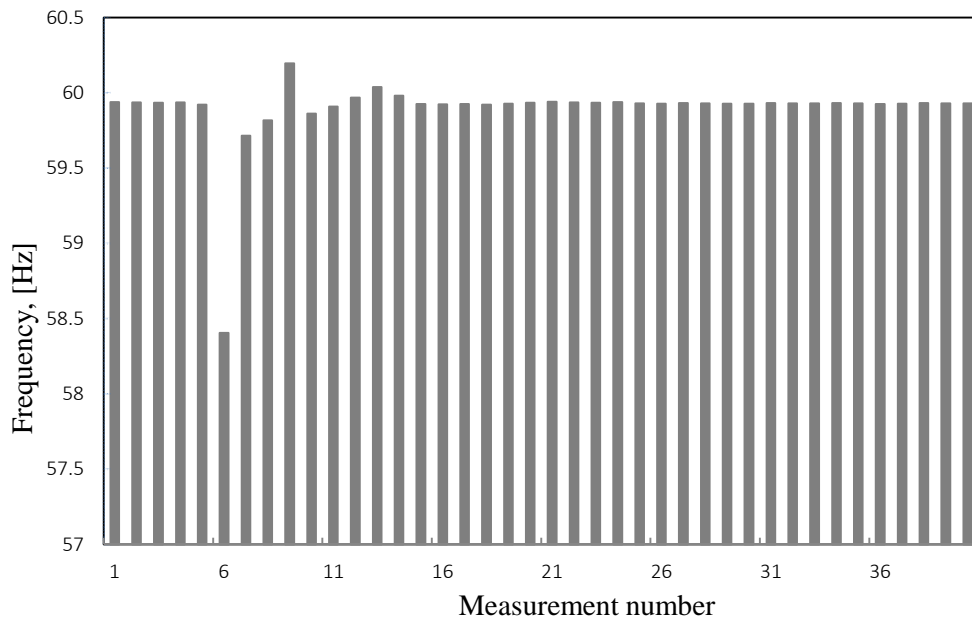


Figure 5.12 Single-cycle measurement window measurements for data including EHV line fault

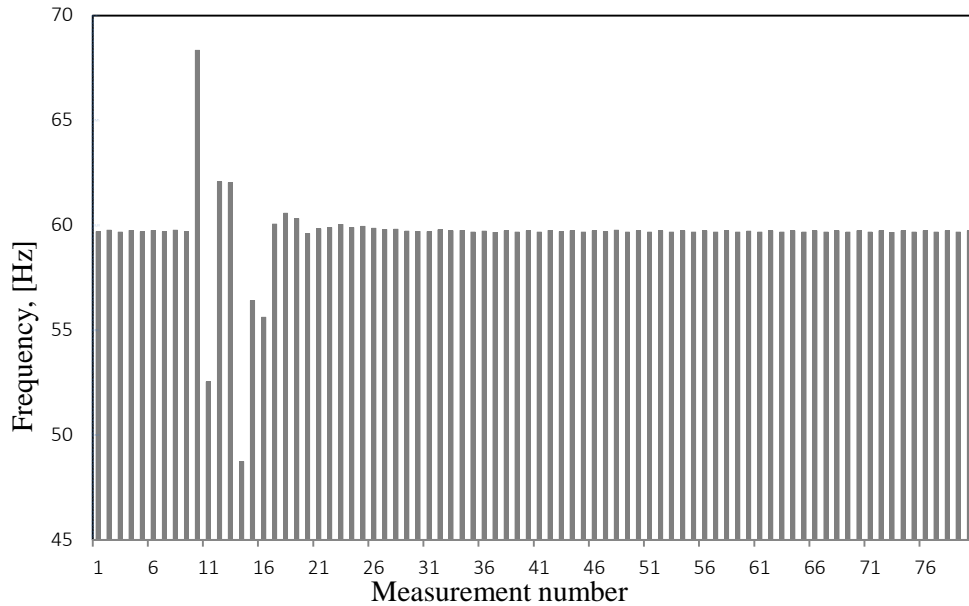


Figure 5.13 Half-cycle measurement window measurements for data including EHV line fault

From Figure 5.13, Figure 5.12, Figure 5.11, and Figure 5.10 the variability is very clear. With the measurement window decreasing we seemingly get more detail, but with half-cycle reported values we also get very high variance over the data where the fault occurred and the frequency at first jumps to 68 Hz and then plummets to 52 Hz giving 16 Hz difference between two adjacent half-cycles, which just does not make sense (not physically possible). Considering the waveform of the fault (given in Figure 5.6) it is more understandable – the signal only vaguely resembles sine-wave, so measurements only vaguely resemble sensible information (when using model of a phasor). With 4-cycle measurements the frequency is seemingly undisturbed by the fault.

It is important at this stage to look at the SEMPR and the meaning of the measurement. First, 52 Hz is what apparently gives the least amount of residuals at that given moment. Second, we are looking for coefficient in a phasor model (6) and by the looks of it, the signal is not a phasor. Our model for representing the nature makes no sense. We get that indication also from GoF that for the measurement producing 52 Hz is 26 dB, instead of steady 44 dB for rest of data set.

It basically doesn't matter whether we use half-cycle or 4-cycle measurements, with wrong underlying mathematical model it will still make little sense. For less variance use longer windows, for more sense (intelligence) use better conceptual models.

Unfortunately, AEP data is not suitable to sensibly represent Allan variance calculations, there simply isn't enough data. Allan variance is, after all, based on the variations from a supposedly stable signal. Larger data chunks were made available by a μ PMU device [29] sampling at 512 samples per cycle and providing 30 seconds worth of data from a medium voltage distribution grid. These data are courtesy of Alex

McEachern of Power Standards Laboratory. For starters, there is a lot of noise and harmonics on the signal, that can be observed in Figure 5.14.

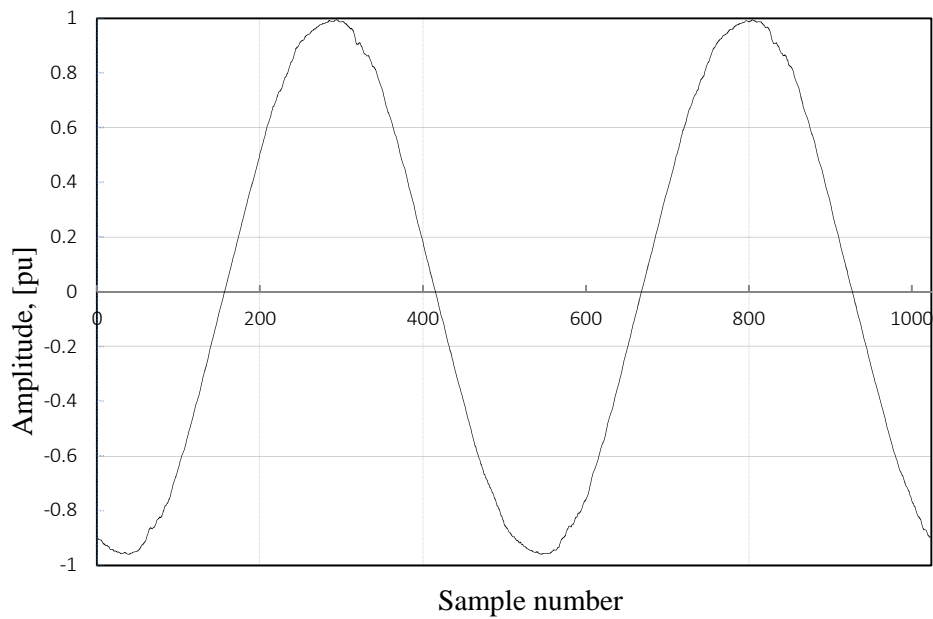


Figure 5.14 uPMU sampled data in MV distribution system

The harmonic content can also be observed in the spectrum of the time series in Figure 5.15

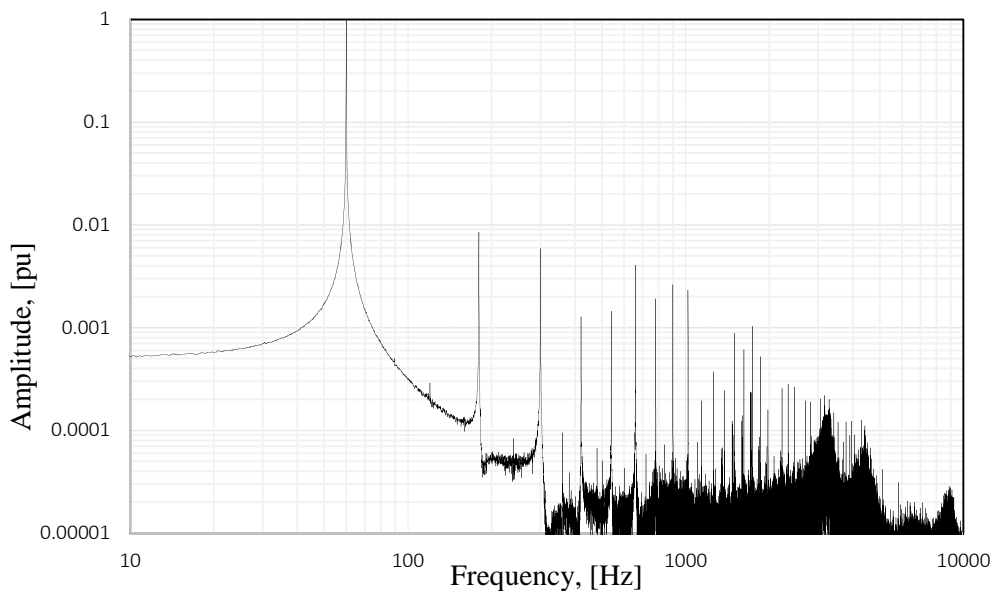


Figure 5.15 Spectrum of the uPMU sampled data

Signal clearly contains 3rd, 5th and 11th harmonic as well as high frequency noise. Since the data set is from normal system operation period, the values should be reasonably stationary and Allan variance can be calculated.

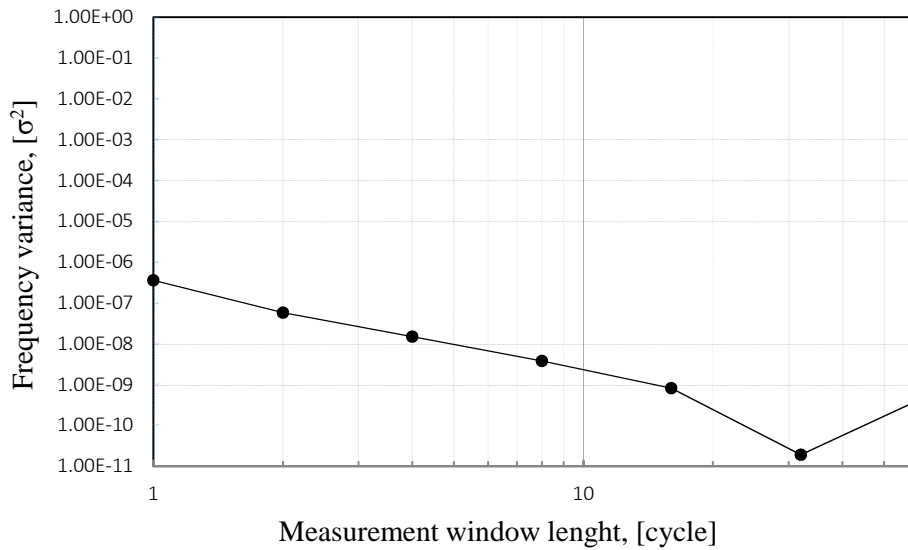


Figure 5.16 Allan variance for distribution network frequency measurements

In Figure 5.16 each dot represents an Allan variance calculated from different number of measurements since the data set is finite. Figure 5.16 shows a distinctive minimum at 32 cycle measurement window, which would give approximately half a second frequency reporting time. Of course, twice per second reporting rate is well below what’s expected from PMU, but also single cycle measurements have very small variance – ppm. It is also worth repeating at this point that SEMPR doesn’t implement any signal filtering.

6 Conclusions

The notion that the process of measurement is in fact the same as solving an equation lends itself well for examination with time-varying signals that can be reasonably modeled, as is expected to be the case for the various power system quantities. The “experiment” of making a measurement by curve-fitting gives results that are similar to the results of other methods, proving that the act of measuring is one that can be done in various ways, but the end result should not depend on the method selected. Most importantly, it teaches that measurement is the act of using signals from the real world to find parameters of a model. That model is almost always a simplification.

Firstly, the notion to separate the conceptual world from nature and reality is very important.

The concept is not new: Maxwell was aware of the need to keep these things separate when he said this in a presentation in 1870 to the British Association:

“I shall only make one more remark on the relation between mathematics and physics. In

themselves, one is an operation of the mind, the other is a dance of molecules.”

Rudolf Carnap [15] stressed the importance of separating the conceptual world and nature in his equation for adding quantities. All this gives the philosophical foundation for the Kirkham model and brings changes in phasor model, calling it “phasor-like” for Phasor Measurement Units (PMUs).

The idea of measurement being the same as solving an equation gives more room for improving and adjusting our conceptual models for reality observed. In this case a Kirkham equation is used instead of just a phasor to show its advantages in real-world applications. This gives PMUs added degrees of freedom for amplitude and frequency to account for time-varying signal that is in power system.

PMUs now are one of the most influential modern measurement devices especially for stability-challenged power systems. For the same system control and supervision targets it could be possible to also use PMUs in distribution network. Of course, strong communication backbone is essential for synchronized measurements.

Research shows that commercial PMUs struggle with signals under transition process. This caused the amending the PMU standard at IEEE. This shouldn't be so, and PMUs must report something. The fundamental problem seems to be that the model used in the solution algorithms is a poor match for the actual signal. How believable are the measurements? What happens when parameters are changing constantly? The commercial PMU does not give any indication.

A metric Goodness of Fit is introduced here and has been integrated in SEMPR. The Goodness of Fit parameter, developed from an idea in [5], has showed potential to be very useful with real PMUs and real signals. It indicates in real time the degree of match between the signal (changing with the power system), and the measurand (fixed by the design of the PMU).

About the Goodness of Fit Metric:

- 1) GoF level can be calculated by any PMU. The calculation is straightforward, and does not depend on the measurement method;
- 2) The Goodness of Fit indicates that near-ideal results can be obtained with an ideal signal;

There is confidence that GoF method will show good results on more real-world data and real-world PMUs than what have already been examined. As mentioned the method offered here is not limited to PMUs. It could be implemented as part of any digital measurement whose measurand equation can be elucidated (an example of double exponent is given in Annex 2). Altogether, GoF is proved to be a promising technique for a large class of digital measurements.

The effect on PMU measurement of different noises has been tested. The results show that Brownian noise has the greatest impact on measurement. There is less impact for white (Gaussian) noise. For harmonics, we can adjust the model and the impact is minimized.

From performed calculations it has been showed that ROCOF is actually a tiny variable in the mathematical model and its contribution to the final signal is down almost to noise levels. More research in noise and its effects on the model could be performed to further improve the ROCOF measurement. It seems quite meaningless before we improve our understanding [54].

As part of the noise assessment, an Allan variance metric was used. This is a statistical analysis tool usually used for precision oscillators. It was found, interestingly, that frequency and ROCOF measurements are sensitive to window lengths (significantly more so than amplitude or phase). Measurement of these quantities would greatly benefit from longer measurement windows.

It has also been found by introducing synthetic semantic coloration (Brownian noise), and based on Allan variance calculations, that an optimum emerges for window lengths. The optimum changes according to the contents of the signal (noise content and amplitude), e.g. for phase measurement with smaller noise amplitudes (up to 1.5% white Gaussian (WG) and 0.3% Brownian (B)) the optimum is around 10 cycles, but for larger amplitudes (up to 15%WG and 1%B) around 2 cycles. For more typical 1.5%WG and 0.03%B noise levels an optimum was found for 512 samples per cycle which is what μ PMU uses in [29].

An additional statistical analysis tool has been proposed called “sampling variance”. It is showed that an optimum value also exists for sampling rate, depending on the signal and noise content. For smaller noise amplitudes (0.5%WG and 0.09%B) the optimum sampling frequency is 384 samples per cycle, but for large noises (15%WG and 1%B) optimum is quite flat around 100 samples per cycle.

The results of this work, looking at real-world data, support the notion that PMU devices are actually solving a phasor equation. The main issue with that is that a lot of time, the power system signals don't perfectly resemble a phasor. The GoF metric shows that Kirkham equation would be better option, since more degrees of freedom are provided for signal to change. Using Kirkham model showed a 6dB increase in GoF (14% increase since steady state GoF is around 43dB) over the fault data.

When variance techniques are applied to obtained real world data, it shows that shorter observation windows are not necessarily more informative than a sensible compromise. Considering small ROCOF signal and high disturbance content on signal during fault, it is actually useless to look at the event through glasses of a phasor. Short (for example half-cycle) measurement windows result in the largest variance.

Statistical analysis is something that PMU also can do just like GoF calculation. In this case it is possible to adjust the conceptual model (including observer notification, of course), window length (possible multiple measurement windows at the same time), sampling frequency to achieve best possible representation of the real signal (maximum GoF value). Such device would perform informed and intelligent measurements providing more information about the nature.

One of the findings is that the noise in the power system is not very researched topic and true nature of the disturbances are still quite unknown. As the matter of fact, also the power system signals under fault conditions are yet to be studied and not only curve fitting but pattern recognition approach may be suggested. This way it would be possible to get better and better GoF values and increase our understanding about the true nature of the physical phenomena in real time (to PMU sense).

Real PMU with GoF integration is under way [55], therefore more data and possible findings are possible. With reported GoF values along declared parameter values will bring knowledge to the observer whether to trust or discard the measurement and in power system operations this is huge improvement.

Underlying principles of intelligent measurements discussed in this work are truly fundamental and affect almost all current day metrology, since it relies on digital measurements. Dr. Kirkham calls it “The third revolution in measurements”, first being directly readable measurement devices, second the digital measurements. An example of double exponent use case is given in Annex 2. There are more, however. Much more.

7 Annexes

Annex No.1 Example of MATLAB code used in SEMPR

```
clear
clc

%Read real world sampling data from a file;

yy = xlsread('Data_file.xlsx',1,'AF292:AF4707');
T = xlsread('Data_file.xlsx',1,'T100:T163');

for i = 1:68
    low = i * 64;

    for n = 1:64;

        p(n) = yy(low+n);

    end
    y = p';

%% Fitting algorithim: 'fit1'.

[xData, yData] = prepareCurveData( T, y );

% Set up fittype and options

ft = fittype( '(a + b*x)*cos(2*pi*c*x+ 2*pi*(d)*x*x +e)+f',
'indepentent', 'x', 'dependent', 'y' ); %Fitting the equation
opts = fitoptions( 'Method', 'NonlinearLeastSquares' ); %Set Method
opts.DiffMaxChange = 0.0001; %Maximum step change
opts.Display = 'Off'; %Disable display option
opts.Lower = [0.5 -100 30 -500 -6.28 -0.5]; %Lower trust region
boundaries
opts.MaxFunEvals = 10000; %Maximum evaluations allowed
opts.MaxIter = 10000; %Maximum iterations
opts.Robust = 'Bisquare'; %Selecting bisquare robust fitting
opts.StartPoint = [1 0 60 0 0 0]; %Starting values for estimation
opts.TolFun = 1e-14; %Termination tolerance for
functiuon
opts.TolX = 1e-14; %Termination tolerance for x
opts.Upper = [1.2 100 110 500 6.28 0.5]; %Upper trust region
boundaries

% Fit model to the data

[fitresult, gof, fitinfo] = fit( xData, yData, ft, opts ); %Export
values from the curvefitting

RMS(i) = 20*log10(1/gof.rmse); %Calculated GoF values
f(i) = fitresult.c; %Frequency values
A(i) = fitresult.a; %Amplitude values
ph(i) = fitresult.e; %Phase values
C_A(i) = fitresult.b; %Rate of Change of Amplitude
values
C_W(i) = fitresult.d; %Rate of Change of Frequeuncy
values
```

```

DC_offset(i) = fitresult.f;           %DC offset values

if RMS(i) < 30;                       %Capture measurement if GOF
indicates a bad fit
    for j = 1:64;
        y1(j) =
(A(i)+C_A(i)*T(j))*cos(2*pi*f(i)*T(j)+ph(i))+DC_offset(i);

    %Reconstruct the estimated signal

    end
    L = 1:64;
    Resid = y - y1';                 %Calculate residuals

    figure (1)                        %Plot the residuals
    bar(L,Resid)
    grid on
    tt = i;

    figure (2)
    plot(L,y,L,y1')
    grid on

    filename = 'Measurements_results1.xlsx'; %Write the results to
file
    xlswrite(filename,y,1,'A1')
    xlswrite(filename,y1',1,'B1')
    xlswrite(filename,Resid,1,'C1')

end

i
    end

%% Plots for data representation

K = [1:64];

figure(3)
plot( K, A)
grid on;
title( 'Amplitude', 'fontsize', 12 )
xlabel( 'Time (s)', 'fontsize', 12 )
ylabel( 'Amplitude (pu)', 'fontsize', 12 )

figure(4)
plot( K, f)
grid on;
title( 'Frequency', 'fontsize', 12 )
xlabel( 'Time (s)', 'fontsize', 12 )
ylabel( 'Frequency (Hz)', 'fontsize', 12 )

figure(5)
plot( K, ph)
grid on;
title( 'Phase', 'fontsize', 12 )
xlabel( 'Time (s)', 'fontsize', 12 )
ylabel( 'phase (rad)', 'fontsize', 12 )

```

```

figure(6)
plot( K, RMS)
grid on;
title( 'Goodness of the fit', 'fontsize', 12 )
xlabel( 'Time (s)', 'fontsize', 12 )
ylabel( 'dB', 'fontsize', 12 )

%-----

%% Data writing to a file

filename = 'Measurements_results.xlsx';
xlswrite(filename,RMS',1,'E1')
xlswrite(filename,K',1,'F1')

filename = 'Measurements_results.xlsx';
xlswrite(filename,RMS',1,'A1')
xlswrite(filename,fn',1,'B1')

xlswrite(filename,An',1,'C1')
xlswrite(filename,phn',1,'D1')
xlswrite(filename,K',1,'E1')
xlswrite(filename,C_An',1,'F1')
xlswrite(filename,C_wn',1,'G1')

xlswrite(filename,yy,1,'H1')
xlswrite(filename,T,1,'I1')

%% Allan Variance calculation -example-

clear
clc

%% INPUT
%Measurement input

SF = 30; %Sampling frequency
l = [1 2 4 10 20 50]; %select window sizes in cycles
MM = 50; %number of measurements

%White noise input

white_noise_volume_all = [0.01]; %Noise amplitude modifier
red_noise_volumes = [0]; %Red noise amplitude modifier

%Harmonics input

Hn = [0]; %Harmonics number
Ha = [0]; %Harmonic amplitudes, pu
Hp = [0]; %harmonics phases, rad

%MATLAB generated signal

Amplitude = 1; %pu
ROCOA = 0; %pu/s
ROCOF = 0; %Hz/s
Frequency = 50; %Hz
phase = 0; %rad

```

```

DC_offset = 0; %pu

%% Measuring algorithm

for r = 1:length(white_noise_volume_all) %Performs measurements
    according to the designated noise volumes

        clearvars yc HH H noise y RMS fn An phn C_wn delta_f delta_phn
        delta_A delta_C_wn %Clearing all previous
        cycle values

        white_noise_volume = white_noise_volume_all(r); %Selects noise
        volume
        red_noise_volume = red_noise_volumes(r); %Selects noise
        volume

    for j = 1:length(l) %Main cycle. Changes window sizes.

        T = 0:( 1 / (SF * 60) ) : (( (l(j) * SF) ) / ( SF * 60 )) - ( 1 / (SF
        * 60) );

        %Constructs appropriate time series for given window length

        for i = 1:MM %Measurement counter

            white_noise = ((1) + ((-1)-1).*rand(1,length(T))) *
            white_noise_volume; %Generates broadband unfiltered noise

            red_noise = (cumsum(randn(1,length(T))))*red_noise_volume;
            %Generates red noise

            noise = white_noise + red_noise; %Final noise signal

            parfor a = 1:length(T) %generate fundamental

                yc(a) = ( Amplitude + ROCOA * T(a)+ noise(a)) * cos( 2 *
                pi * Frequency * T(a) + 2 * pi * ROCOF * T(a) * T(a) + phase ) +
                DC_offset; %Generates the fundamental with Kirkham
                equation +noise

            end

            HH = zeros(1,length(T)); %generates harmonics signal

        for u = 1:length(Hn) %loop for harmonics generation

            parfor a = 1:length(T)

                H(a) = (Ha(u)) * cos( 2 * pi * 60 * Hn(u) * T(a) + Hp(u) );
                %generates harmonics with phasor equation

            end

            HH = HH + H; %all harmonics added together

        end

    end
end

```

```

        y = yc + HH;                                %Final input signal

%% Fit: 'fit1'.

[xData, yData] = prepareCurveData( T, y ); %preparing data for curve
fitting

% Set up fittype and options

ft = fittype( '(a + b*x)*cos(2*pi*c*x+ 2*pi*(d)*x*x +e)+f',
'indepentent', 'x', 'dependent', 'y' ); %Fitting the equation
opts = fitoptions( 'Method', 'NonlinearLeastSquares' ); %Set Method
opts.DiffMaxChange = 0.0001; %Maximum step change
opts.Display = 'Off'; %Disable display option
opts.Lower = [0.5 -100 30 -500 -6.28 -0.5]; %Lower trust region
boundaries
opts.MaxFunEvals = 10000; %Maximum evaluations
allowed
opts.MaxIter = 10000; %Maximum iterations
opts.Robust = 'Bisquare'; %Selecting bisquare
robust fitting
opts.StartPoint = [1 0 60 0 0 0]; %Starting values for
estimation
opts.TolFun = 1e-14; %Termination tolerance
for functiuon
opts.TolX = 1e-14; %Termination tolerance
for x
opts.Upper = [1.2 100 110 500 6.28 0.5]; %Upper trust region
boundaries

% Fit model to the data
[fitresult, gof, fitinfo] = fit( xData, yData, ft, opts ); %Export
values from the curvefitting

RMS(i) = 20*log10(1/gof.rmse); %Calculated GoF values
f(i) = fitresult.c; %Frequency values
A(i) = fitresult.a; %Amplitude values
ph(i) = fitresult.e; %Phase values
C_A(i) = fitresult.b; %Rate of Change of
Amplitude values
C_W(i) = fitresult.d; %Rate of Change of
Frequeuncy values
DC_offset(i) = fitresult.f; %DC offset values

if i > 1; %Calculate the differences in
measurements for Allan variance calculation

    delta_f(i) = (f(i) - f(i-1))^2; %frequency differences
    delta_ph(i) = (ph(i) - ph(i-1))^2; %phase differences
    delta_A(i) = (A(i) - A(i-1))^2; %amplitude differences
    delta_C_A(i) = (C_A(i) - C_A(i-1)); %ROCOA differences
    delta_C_W(i) = (C_W(i) - C_W(i-1)); %ROCOF differences
end

end

%Allan variance calculation and vector assembly

Allan_variance_f(r,j) = (sum(delta_f))/(2*(i-1));

```

```

Allan_variance_ph(r,j) = (sum(delta_ph))/(2*(i-1));
Allan_variance_A(r,j) = (sum(delta_A))/(2*(i-1));
Allan_C_A(r,j) = (((sum(delta_C_A))/(i-2))^2)/2;
Allan_C_W(r,j) = (((sum(delta_C_w))/(i-2))^2)/2;
Avg_GoF(r,j) = mean(RMS);           %Average GoF values

%% Write to the Excel file

filename = 'Alan_variance.xlsx';

xlswrite(filename,f',(1+j),'A2')
xlswrite(filename,A',(1+j),'B2')
xlswrite(filename,ph',(1+j),'C2')
xlswrite(filename,C_W',(1+j),'D2')
xlswrite(filename,RMS',(1+j),'E2')

end

end

%% Allan deviance

Allan_deviance_f = sqrt(Allan_variance_f);
Allan_deviance_ph = sqrt(Allan_variance_ph);
Allan_deviance_A = sqrt(Allan_variance_A);

```

Annex No. 2 An Example of a Double Exponent Signal Estimation

Mathematical model for double exponent:

$$V(t) = V e^{\frac{-t}{\alpha}} - e^{\frac{-t}{\beta}}, \quad (1)$$

Where time constant α establishes the rise of the impulse and β accordingly the fall of the impulse. With $\alpha=0.02$ and $\beta=5$ the signal; is given in Figure1.

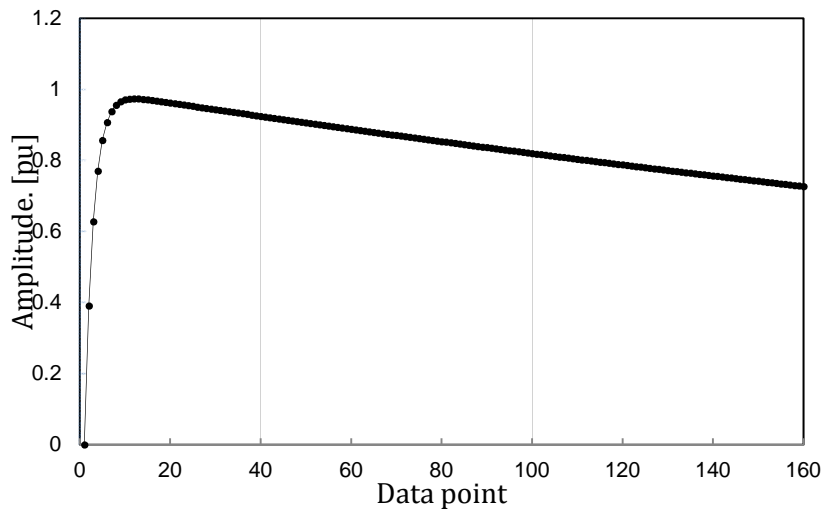


Figure1. A synthetic double exponent signal.

For clean signals SEMPR can estimate the values perfectly, which is shown in residuals below in Figure2.

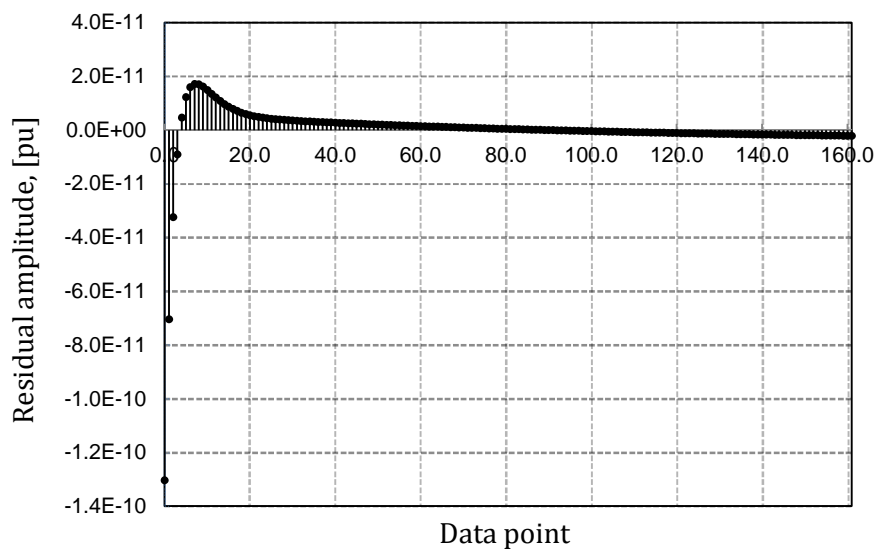


Figure2. Residuals from generated and reconstructed signals.

With introduced 3% white Gaussian noise the signal and residuals are given in Figure3 and Figure4.

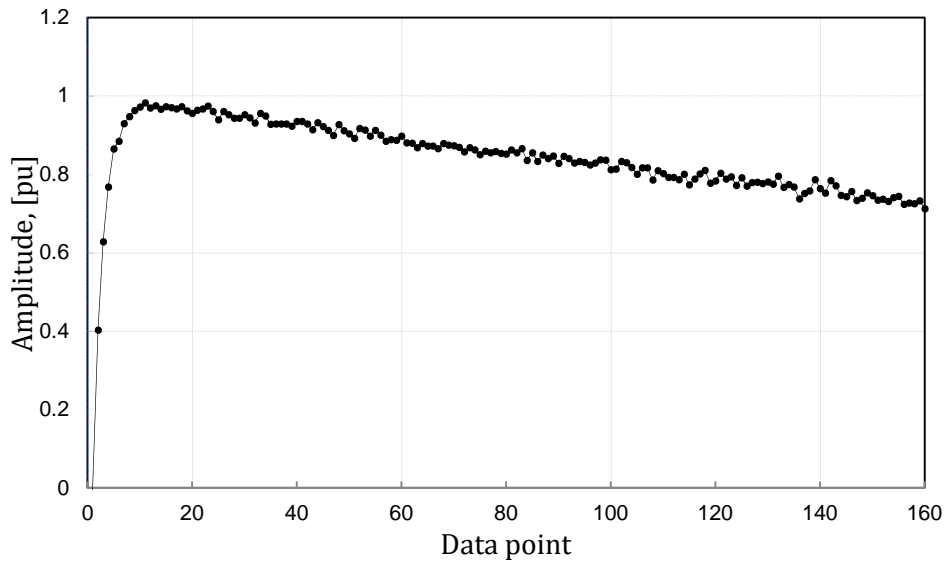


Figure3. Double exponent signal with introduced 3% white Gaussian noise.

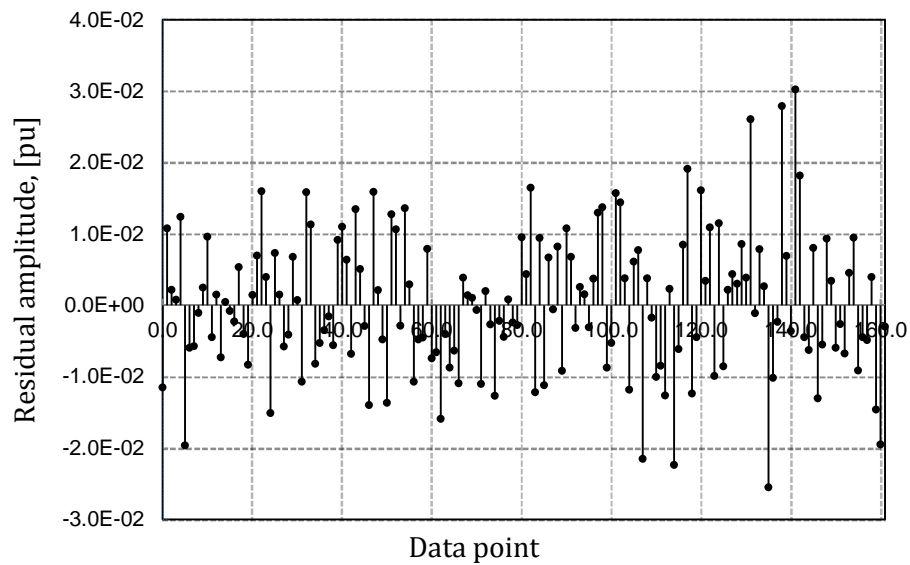


Figure4. Residuals from generated signal and reconstructed signal.

The residuals are practically the same as the noise signal, showing that SEMPR can indeed estimate different mathematical models in presence of noise (approximately 0.4% of the noise signal actually contributed to the parameters estimation).

Annex No. 3 representational measurements

There are many ways to measure frequency:

- Count zero crossings
- Fourier analysis
- Measure zero crossing intervals
- Finite difference phase values.

But these are ways to measure, not descriptions of what we measure. They do not define the quantity being measured, the thing called “frequency.”

In fact, the IEEE Standard [1] does not define the thing being measured except via a textbook kind of definition, one that assumes constant frequency. There seems not to be a good definition of the word frequency that applies when the frequency is changing. The definition can be different for different measurement methods, like Apparent Local Frequency for SEMPR, which can indeed be defined.

What this means is that the PMU is actually measuring something that is not defined. As a result, the value that is obtained as the result of the measurement depends on the details of how the measurement is performed.

As it happens, this kind of measurement is more common than is generally realized. Many measurements give results that depend critically on the way the measuring is done” air temperature (quoted on weather reports) is a common example. It can be measured as the level of mercury in glass tube with no reference to what “temperature” means in physics.

Measurements of this kind are known as operationalist (because the operation of measurement must be followed exactly for the result to be useful) and the kind of measurement that we imagine we are usually making is known as representational, because (following Carnap) the way the physical quantities are thought to interact is represented by the way the mathematical quantities interact. [56]

In power systems, there are many quantities that are measured operationally. An example that is simple to see as operational is that of partial discharge. The way the measurement is to be carried out is very closely defined in the standard [57]. The bandwidth of the input filter is specified, the kind of detector, and some filtering of the output.

The measurement of frequency in the PMU is a measurement of this kind, though it is not generally recognized. The IEEE Standard contains a good deal of descriptions of filtering before and after the measurement is made, for example.

SEMPR was an attempt to make a measurement that was as representational as possible. By adding a term in the rate-of-change-of frequency to the sinusoid equation, the model was thought to be a representation of the actual power system. In fact,

because the power system typically contains harmonics, the fitting process is limited in accuracy unless the harmonics are accounted for. If the harmonics are filtered out, the measurement is more operational. If the harmonics are included in the SEMPR objective function, the measurement is more representational.

As the model complexity increases, it may at some point be computationally impractical to solve the fitting problem. Kirkham is continuing to work on this at PNNL.

8 References

- [1] IEEE Power and Energy Society, "IEEE Std C37.118.1a-2014 Modification of Selected Performance Requirements," 2014.
- [2] Gerard Stenbakken, Ming Zhou, "Dynamic Phasor Measurement Unit Test System," in *Power Engineering Society General Meeting*, Tampa, USA, 2007.
- [3] A.Riepnieks, H.Kirkham, L.Ribickis, "Considerations for Phasor Measurement Unit Introduction in Distribution System," in *56th International Scientific Conference on Power and Electrical Engineering of RTU*, Riga, Latvia, 2015.
- [4] A. Riepnieks, H. Kirkham, "Rate of change of frequency measurement," in *Power and Electrical Engineering of Riga Technical University (RTU CON)*, Riga, 2016.
- [5] A.Riepnieks, H.Kirkham, "An Introduction to Goodness of Fit for PMU Parameter Estimation," *IEEE Transactions on Power Delivery*, vol. 32, no. 5, pp. 2238-2245, 2017.
- [6] A.Riepnieks, H.Kirkham, A.J.Faris, M.Engels, "Phase jumps in PMU signal generators," in *2017 IEEE Power & Energy Society General Meeting*, Chicago, USA, 2017.
- [7] H.Kirkham, A.Riepnieks, "Dealing with non-stationary signals: Definitions, considerations and practical implications," in *Power and Energy Society General Meeting*, Boston, USA, 2016.
- [8] H.Kirkham, A.Riepnieks, "Students' simple method for determining the parameters of an AC signal," in *2016 57th International Scientific Conference on Power and Electrical Engineering of Riga Technical University (RTU CON)*, Riga, Latvia, 2016.
- [9] H.Kirkham, A.Riepnieks, E.So, J.McBride, "Error correction: A proposal for a standard," in *2016 Conference on Precision Electromagnetic Measurements*, Ottawa, Canada, 2016.
- [10] H.Kirkham, A.Riepnieks, M.Albu, D.Laverty, "The nature of measurement, and the true value of a measured quantity," in *2018 IEEE International Instrumentation and Measurement Technology Conference*, Houston, USA, 2018.
- [11] Harold Kirkham, Artis Riepnieks, "Measurement of Phasor-like Signals," Pacific Northwest National Laboratory, Richland, USA, 2016.
- [12] Conseil Européen pour la Recherche Nucléaire, "The Standard Model," CERN, 2018. [Online]. Available: <https://home.cern/about/physics/standard-model>. [Accessed 2018].

- [13] A.Mazer, *Shifting the Earth: The Mathematical Quest to Understand the Motion of the Universe*, New Jersey, USA: A John Wiley & Sons Inc., 2011.
- [14] The Regents of The University of California, "Rudolf Carnap, Philosophy: Los Angeles," 2011. [Online]. Available: <http://texts.cdlib.org/view?docId=hb6h4nb3q7&doc.view=frames&chunk.id=div00004&toc.depth=1&toc.id=.> [Accessed 2018].
- [15] R. Carnap, *Philosophical Foundations of Physics*, New York, USA: Basic Books Inc., 1966.
- [16] J. Rutman, "Characterization of phase and frequency instabilities in precision frequency sources: Fifteen years of progress," *Proceedings of the IEEE*, vol. vol.66, no. 9, 1978.
- [17] J. Rutman, "Oscillator Specifications: a Review of Classical and New Ideas," in *31st Annual Symposium on Frequency Control*, Atlantic City, USA, 1977.
- [18] C. Shannon, "A mathematical theory of communication," *The Bell System Technical Journal*, vol. Vol.27, no. 4, pp. 623-656, 1948.
- [19] A. K.Srivastava, Writer, *Phasor Measurement (Estimation) Units*. [Performance]. Washington State University, 2013.
- [20] A. Phadke, "Synchronized phasor measurements in power systems," *IEEE Computer Applications in Power*, vol. 6, no. 2, pp. 10-15, 1993.
- [21] R. d. Vries, Writer, *Phasor Measurement Units (PMUs) and time Synchronization at European Utilities*. [Performance]. Arbiter, 2013.
- [22] D.Antonovs, A.Sauhats, A.Utans, A.Svalovs, G.Bochkarjova, "Protection scheme against out-of-step condition based on synchronized measurements," in *2014 Power Systems Computation Conference*, Wroclaw, Poland , 2014.
- [23] A.Sauhats, I.Svalova, A.Svalovs, D.Antonovs, A.Utans, G.Bochkarjova, "Two-terminal out-of-step protection for multi-machine grids using synchronised measurements," in *2015 IEEE Eindhoven PowerTech*, Eindhoven, Netherlands, 2015.
- [24] Yong Li, Dechang Yang, Fang Liu, Yijia Cao, Christian Rehtanz, *Interconnected Power Systems: Wide-Area Dynamic Monitoring and Control Applications*, Springer, 2015.
- [25] Raymond H.Byrne, Ricky J. Concepcion, Jason Neely, "Small signal stability of the western North American power grid with high penetrations of renewable generation," in *Photovoltaic Specialists Conference (PVSC)*, Portland, 2016.
- [26] Project Group Turkey, "Report on Blackout in Turkey on 31st March 2015," European Network of Transmission System Operators for Electricity, Brussels, 2015.

- [27] "IEEE Std. C37.118.1-2011 Standard for Synchrophasor Measurements for Power Systems," *IEEE Standard*, 2011.
- [28] A.G. Phadke, J.S. Thorp, M.G. Adamiak, "A new Measurement Technique for Tracking Voltage Phasors, Local System Frequency, and Rate of Change of Frequency," *IEEE Transactions on Power Apparatus and Systems*, Vols. PAS-102, no. 5, pp. 1025-1038, 1983.
- [29] A. von Meier, D. Culler, A. McEachern, "Micro-synchrophasors for distribution systems," in *Innovative Smart Grid Technologies Conference (ISGT)*, Washington DC, 2014.
- [30] K. Gheen, Writer, *Phase Noise Measurement Methods and Techniques*. [Performance]. Agilent Technologies, 2012.
- [31] W. Dickerson, "Effect of PMU analog input section performance on frequency and ROCOF estimation error," in *IEEE International Workshop on Applied Measurements for Power Systems*, Aachen, Germany, 2015.
- [32] A. Goldstein, Writer, *Lessons learned from the NIST assessment of PMUs*. [Performance]. National Institute of Standards and Technology, 2014.
- [33] B. v. d. Pol, "The Fundamental Principles of Frequency Modulation," *Journal of the Institution of Electrical Engineers - Part III: Radio and Communication Engineering*, vol. Vol.93, no. 23, pp. 153-158, 1946.
- [34] B. Boashash, "Estimating and interpreting the instantaneous frequency of a signal. I. Fundamentals," *Proceedings of the IEEE*, vol. vol.80, no. 4, 1992.
- [35] Jacques Rutman, F.L.Walls, "Characterization of Frequency Stability in Precision Frequency Sources," *Proceedings of the IEEE*, vol. 79, no. 6, 1991.
- [36] H.Kirkham, J.Dagle, Y.Sun, "PMU Measurement Technology," Pacific Northwest National Laboratory, Richland, USA, 2014.
- [37] H. Kirkham, "A conceptual Framework for Measurement (with emphasis on phasor measurement)," Pacific Northwest National Laboratory, Richland, USA, 2015.
- [38] W.Heisenberg, *Physics and Philosophy: The Revolution in Modern Science*, London: George Allen and Unwin, 1959.
- [39] T. M. Inc., ""Documentation",," 2018. [Online]. Available: <http://www.mathworks.com/help/matlab/>.
- [40] Joint Committee for Guides in Metrology, *Evaluation of measurement data - Guide to the expression of uncertainty in measurement*, Bureau International des Poids et Mesures, 2008.

- [41] D.Cuthbert, F.S. Wood, *Fitting Equations to Data*, New York, USA: Wiley, 1971.
- [42] N. Shah, "Whitepaper: Harmonics in power system. Causes, effects and control," May 2013. [Online]. Available: <https://www.industry.usa.siemens.com>. [Accessed 2018].
- [43] D. Allan, "Time and Frequency (Time-Domain) Characterization, Estimation, and Prediction of Precision Clocks and Oscillators," *IEEE Transactions on Ultrasonics, Ferroelectrics, and Frequency control*, vol. 34, no. 6, pp. 647-654, 1987.
- [44] D. W. Allan, "Statistics of atomic frequency standards," *Proceedings of the IEEE*, vol. 54, no. 2, pp. 221-230, 1966.
- [45] David W. Allan, Neil Ashby, Cliff Hodge, "The Science of Timekeeping," Hewlett-Packard Company, 1997.
- [46] R.Torres, Z.Lizarazo, E.Torres, "Fractional Sampling Theorem for -Bandlimited Random Signals and Its Relation to the von Neumann Ergodic Theorem," *IEEE Transactions on Signal Processing*, vol. Vol.62, no. 14, pp. 3695-3705, 2014.
- [47] W. Splettstober, "Error Analysis in the Walsh Sampling Theorem," in *1980 IEEE International Symposium on Electromagnetic Compatibility*, Baltimore, 1980.
- [48] J.Zhai, L.Zhang, Z.Yu, "Digital predistortion of RF power amplifiers with Zhu's general sampling theorem," in *2015 Asia-Pacific Microwave Conference*, Nanjing, 2015.
- [49] H. Nyquist, "Certain Topics in Telegraph Transmission Theory," *Transactions of the American Institute of Electrical Engineers*, vol. Vol.47, no. 2, pp. 617-644, 1928.
- [50] C. Shannon, "Communcation in the Presence of Noise," *Proceedings of the IRE*, vol. Vol.37, no. 1, pp. 10-21, 1949.
- [51] G.D'Antona and A.Ferrero, *Digital Signal Processing for Measurement Systems: Theory and Applications*, Springer, 2006.
- [52] T. Wescott, "Sampling: What Nyquist Didn't Say, and What to," Wescott Design Services, 2016.
- [53] K. J. Åström, "On the Choice of sampling rates in Parametric Identification of Time Series," Lund Institute of Technology division of automatic control, Lund, Sweden, 1968.
- [54] H. Kirkham, S. Pandey, "Is ROCOF measurable?," in *2018 IEEE Power & Energy Society Innovative Smart Grid Technologies Conference (ISGT)*, Washington, USA, 2018.

- [55] D.M. Lavery, H. Kirkham, D.J. Morrow, X. Liu, "Estimation of goodness of fit of synchrophasors during transient faults," in *2017 IEEE Power & Energy Society General Meeting*, Chicago, USA, 2017.
- [56] D. Hand, *Measurement Theory and Practice*, London: Arnold, 2004.
- [57] IEC, "IEC 60270 High-voltage test techniques – Partial Discharge Measurements," International Electrotechnical Commission, Geneva, Switzerland, 2000.
- [58] IEEE Standard Definitions for the Measurement of Electric Power Quantities Under Sinusoidal, Nonsinusoidal, Balanced, or Unbalanced Conditions, New York: IEEE Power & Energy Society , 2010.
- [59] B. v. d. Pol, "The Fundamental Principles of Frequency Modulation," *Journal of the Institution of Electrical Engineers - Part III: Radio and Communication Engineering*, vol. Vol. 93, no. 23, pp. 153-156, 1946.
- [60] International Electrotechnical Commission, IEC 60270 High-voltage test techniques – Partial Discharge Measurements, Geneva, Switzerland: IEC, 2000, p. 99.